HHS Public Access

Author manuscript

Methods Enzymol. Author manuscript; available in PMC 2025 August 28.

Published in final edited form as:

Methods Enzymol. 2024 ; 705: 271–309. doi:10.1016/bs.mie.2024.08.002.

Direct, ensemble FRET approaches to monitor transient state kinetics of human DNA polymerase δ holoenzyme assembly and initiation of DNA synthesis

Jessica L. Norris, **Mark Hedglin***

Department of Chemistry, The Pennsylvania State University, University Park, PA, United States

Abstract

In humans, DNA polymerase δ (pol δ) holoenzymes, comprised of pol δ and the processivity sliding clamp, proliferating cell nuclear antigen (PCNA), carry out DNA synthesis during lagging strand replication, the initiation of leading strand DNA replication as well as most of the major DNA damage repair pathways. In each of these contexts, pol δ holoenzymes are assembled at primer/template (P/T) junctions and initiate DNA synthesis in a stepwise process that involves the PCNA clamp loader, replication factor C and, depending on the DNA synthesis pathway, the major single strand DNA-binding protein complex, replication protein A (RPA). In a recent report from our laboratory, we designed and utilized direct, ensemble Förster Resonance Energy Transfer approaches to monitor the transient state kinetics of pol δ holoenzyme assembly and initiation of DNA synthesis on P/T junctions engaged by RPA. In this chapter, we detail the original approaches and discuss adaptations that can be utilized to monitor fast kinetic reactions in the millisecond (ms) timescale. All approaches described in this chapter utilize a commercially-available fluorescence spectrophotometer, can be readily evolved for alternative DNA polymerases and P/T DNA substrates, and permit incorporation of protein posttranslational modifications, accessory factors, DNA covalent modifications, accessory factors, enzymes, etc. Hence, these approaches are widely accessible and broadly applicable for characterizing DNA polymerase holoenzyme assembly and initiation of DNA synthesis during any PCNA-dependent DNA synthesis pathway.

1. Introduction

In humans, DNA polymerase δ (pol δ) holoenzymes, comprised of pol δ and the processivity sliding clamp, proliferating cell nuclear antigen (PCNA), carry out DNA synthesis during lagging strand replication (Clausen et al., 2015; Hedglin & Benkovic, 2017a; Lujan et al., 2016; Miyabe et al., 2011; Nick McElhinny et al., 2008), the initiation of leading strand DNA replication (Zhou et al., 2019) as well as many of the major DNA damage repair pathways, such as long-patch base excision repair (Robertson et al., 2009), nucleotide excision repair (NER) (Spivak, 2015), mismatch repair (MMR)(Modrich, 2016), and homologous recombination pathways (Donnianni et al., 2019; Lydeard et al., 2007; Maloisel et al., 2008; Wilson et al., 2013; Zhang et al., 2023). In each of these contexts, pol δ

*Corresponding author. muh218@psu.edu.

holoenzymes are assembled at primer/template (P/T) junctions and initiate DNA synthesis in a stepwise process that involves the PCNA clamp loader, replication factor C (RFC) and, depending on the DNA synthesis pathway, the major single strand DNA (ssDNA)-binding protein complex, replication protein A (RPA) (Hedglin & Kumar et al., 2013; Hedglin et al., 2016; Hedglin & Perumal et al., 2013; Kim et al., 1994; Kim et al., 1992; Kim & Wold, 1995; Kolinjivadi et al., 2017; Kolpashchikov et al., 2001; Kolpashchikov et al., 1999; Pestryakov et al., 2004; Pestryakov et al., 2003). In short, RFC utilizes ATP to "load" PCNA onto the respective P/T junction such that the "front face" of PCNA is oriented towards the 3′ hydroxyl (OH) terminus of the primer strand (Hedglin & Benkovic, 2017b; Hedglin & Kumar et al., 2013; Hedglin & Perumal et al., 2013; Yuzhakov et al., 1999). After completion of PCNA loading, the resident RPA stabilizes loaded PCNA at/near the P/T junction by prohibiting RFC-catalyzed unloading of PCNA and diffusion of PCNA along the adjacent ssDNA (Hedglin & Benkovic, 2017b). Diffusion of loaded PCNA along the upstream double-strand DNA (dsDNA) region is restricted by engaged "protein roadblocks," such as nucleosomes and high-affinity transcription factors (Fennessy & Owen-Hughes, 2016; Shibahara & Stillman, 1999; Smith & Whitehouse, 2012). Next, pol δ engages the P/T junction and the "front face" of the resident PCNA (forming a holoenzyme), aligns an incoming, complementary dNTP for incorporation at the 3′ OH terminus of the primer strand, and initiates DNA synthesis (Hedglin & Benkovic, 2017b; Lancey et al., 2020; Tsurimoto & Stillman, 1991).

In lagging strand replication, the initiation of leading strand replication, NER, and MMR, pol δ holoenzymes are assembled on P/T DNA substrates that contain ssDNA "gaps" adjacent to the P/T junction from which DNA synthesis initiates from Fig. 1. The ssDNA gaps are ~ 30–150 nucleotides (nt) in length or longer and terminate downstream of the P/T junction in unique structures (Balakrishnan & Bambara, 2013; Fang & Modrich, 1993; Kemp & Hu, 2017; Maloisel et al., 2008; Zhou et al., 2019).[1] RPA engages the entire lengths of the ssDNA gaps in an orientation-specific manner and also directly contacts the 3′ hydroxyl terminus of the primer strand (Kim et al., 1994; Kim et al., 1992; Kim & Wold, 1995; Kolinjivadi et al., 2017; Kolpashchikov et al., 2001; Kolpashchikov et al., 1999; Pestryakov et al., 2004; Pestryakov et al., 2003). In a recent report from our laboratory, we designed and utilized direct, ensemble Förster Resonance Energy Transfer (FRET) approaches to decipher how pol δ holoenzymes are assembled on and initiate DNA synthesis from P/T junctions engaged by RPA. Results from these novel approaches revealed that, throughout this entire process, RPA remains engaged with template ssDNA ~ 6–12 nt downstream of the P/T junction and the RPA•DNA complex dynamically re-organizes to allow successive binding of RFC and pol δ to the 3′ hydroxyl terminus of the primer strand and the template ssDNA immediately adjacent to the P/T junction (Fig. 2) (Norris et al., 2024). The persistent RPA•ssDNA interactions near the P/T junction increase the efficiency of pol δ holoenzyme assembly and the initiation of DNA synthesis by prohibiting diffusion of loaded PCNA along the template ssDNA as well as RFC-catalyzed unloading of PCNA from DNA (Hedglin et al., 2017; Hedglin & Benkovic, 2017b).

[1]For detailed information on how these DNA structures are generated within each of these pathways, readers are directed to the cited review articles.

In this chapter, we detail the direct, ensemble FRET approaches we recently developed to monitor the transient-state kinetics of PCNA loading by RFC, pol δ holoenzyme assembly, and the initiation of DNA synthesis on P/T junctions engaged by RPA (Norris et al., 2024). Furthermore, we discuss adaptations of the original approaches that can be utilized to monitor fast kinetic reactions in the millisecond (ms) timescale. All approaches described in this chapter utilize a commercially-available fluorescence spectrophotometer, can be readily evolved for alternative DNA polymerases and P/T DNA substrates, and permit incorporation of protein posttranslational modifications, accessory factors, DNA covalent modifications, accessory factors, enzymes, etc. Hence, these approaches are widely accessible and broadly applicable for characterizing DNA polymerase holoenzyme assembly and initiation of DNA synthesis during any PCNA-dependent DNA synthesis pathway.

2. Transient-state FRET techniques: A general overview

Transient-state (i.e., non-equilibrium, pre-steady state) FRET has proven to be a very powerful and versatile technique to probe the kinetics and structural dynamics of protein-DNA interactions. A variety of fluorescence molecules can be used in this technique as donor and acceptor FRET pairs but Cyanine 3 (Cy3)/Cyanine 5 (Cy5) is the most widely utilized FRET pair due to the higher photostability and wider spectral separation of these fluorophores (Blouin et al., 2009, 2015).[2] Commonly, a given DNA substrate is site-specifically labeled with a Cy3 donor and a corresponding DNA-binding protein of interest is site-specifically labeled with a Cy5 acceptor. To monitor the protein-DNA interaction over time via intermolecular FRET, the Cy3 donor is directly and continuously excited at a wavelength (typically 514 or 532 nm) that minimally overlaps the excitation spectrum of the Cy5 acceptor and the emission intensities are continuously monitored in a manner that isolates the fluorescence emitted by the Cy3 donor and Cy5 acceptor from each other.

Absorption of a photon by the Cy3 donor elevates an electron to an excited state which then subsequently decays back to the ground state by a combination of competing processes, including emission of a photon (with a peak emission intensity wavelength of 563 nm) and FRET to a Cy5 acceptor. The latter only occurs if the Cy5 acceptor is in close proximity of the excited Cy3 donor (~ < 10 nm). FRET from an excited Cy3 donor to a nearby Cy5 acceptor elevates an electron in the latter to an excited state which then subsequently decays back to the ground state by a combination of competing processes, including emission of a photon (with a peak emission intensity wavelength of 665 nm) (Blouin et al., 2009, 2015).[3] Thus, for a Cy3/Cy5 FRET pair, the gain and loss of FRET over time are directly indicated only by simultaneous, anti-correlated changes in the fluorescence emission intensities of the Cy3 donor and the Cy5 acceptor. Specifically, appearance of (or increase in) FRET is indicated by a decrease (i.e., quenching) in the fluorescence emission intensity of the Cy3 donor together with a simultaneous increase in sensitized Cy5 acceptor fluorescence emission intensity. Likewise, disappearance of (or decrease in) FRET is indicated by

[2]For general considerations of FRET donor-acceptor pairs and experimental designs for investigating protein-DNA interactions, readers are directed to one of the many excellent reviews in the literature, such as the cited references.
[3]For more details on the basic biophysical principles underlying FRET, readers are directed to one of the many excellent reviews in the literature, such as the cited references.

a decrease in sensitized Cy5 acceptor fluorescence emission intensity together with a simultaneous increase (i.e., de-quenching) of Cy3 donor fluorescence emission intensity. Accordingly, and as alluded to above, the direct observance and subsequent quantification of intermolecular FRET over time requires a means to isolate and continuously and simultaneously record the fluorescence emission intensities of the Cy3 donor and Cy5 acceptor over time. This is achieved through multiple approaches/instruments, each with their own advantages, drawbacks, and limitations.

Single molecule (sm) total internal reflection FRET (TIRF) microscopy (smTIRF) is widely used to monitor protein•DNA interactions. In this approach, a reagent is immobilized on a microscope slide surface, another reagent is introduced to initiate a binding interaction, and FRET is directly monitored over time for individual immobilized molecules. Specifically, a large area of the microscope slide surface is excited at a given wavelength by a particular solid-state laser and mirrors and appropriate filters are utilized to record the fluorescence emission intensities of the donor and acceptor dyes simultaneously in distinct emission detection channels. In this approach, fluorescence emissions intensities and, hence, FRET can be recorded at the instant the second reagent is introduced. By monitoring FRET for individual molecules, smTIRF is a very powerful approach that allows for quantitative assessment of structural dynamics and heterogeneity of conformational and kinetic ensembles (Roy et al., 2008).[4] However, the observation times for Cy3/Cy5 FRET pairs are limited to the seconds time scale due to deleterious fluorophore photophysics and/or photochemistry (i.e., “photobleaching”) that are amplified by the high intensity laser power and rapid excitation rates (Cooper et al., 2013). Stopped-flow mixing (i.e., stopped-flow) instruments may also be utilized to monitor protein•DNA interactions via FRET. In this approach, pressured drives rapidly flow two reagent solutions, each contained in separate drive syringes, into a mixing chamber to initiate a binding interaction. The resultant mixture is subsequently flowed into an observation chamber, the flow is stopped, and FRET is directly monitored over time. Specifically, a relatively low intensity Xenon lamp coupled with an excitation monochromator excites the mixture in the observation chamber at a particular wavelength and appropriate filters are utilized to record the fluorescence emission intensities of the donor and acceptor dyes simultaneously in distinct emission detection channels. The time interval between mixing of the reagent solutions in the mixing chamber and the beginning of the fluorescence intensities recordings in the observation chamber is typically < 2 ms and is referred to as the “dead time.” In this approach, FRET can be monitored over very long time intervals (minutes to hours) due to the low intensity xenon lamp power. In general, stopped-flow mixing is a useful approach to study the transient state kinetics of protein•DNA interactions on the ms time scale within an ensemble (Zheng et al., 2015). However, dual-detection channel stopped-flow instruments are currently limited in their capacity to monitor FRET between Cy3/Cy5 donor/acceptor pairs. Specifically, time-dependent traces of Cy3 fluorescence emission intensities are very noisy due to the substantial background of stray excitation light in the Cy3 emission detection channel (Tims & Widom, 2007).

[4]For more details on the design, execution, and analysis of smTIRF experiments, readers are directed to one of the many excellent reviews in the literature, such as the cited references.

In a recent study, we utilized a Duetta-Bio spectrofluorometer (Horiba) to monitor protein•DNA interactions via FRET (Norris et al., 2024). In this approach, a binding reaction is initiated by rapidly mixing two reagent solutions in a cuvette via aliquoting and FRET is directly monitored over time. Specifically, a low intensity 75 W Xenon arc lamp coupled with an excitation monochromator excites the mixture in the cuvette at a particular wavelength and an emission monochromator is utilized to record the fluorescence emission intensities of the donor and acceptor dyes, each at unique wavelengths, essentially simultaneously ($\Delta t_I = 0.118$ ms). The time interval between mixing of the reagent solutions in the cuvette and the beginning of the fluorescence intensities recordings (i.e., "dead time") is ≤10 s. In this approach, FRET between Cy3/Cy5 donor/acceptor pairs can be directly monitored over very long time intervals (minutes to hours) due to the low intensity Xenon lamp power. Furthermore, this approach permits successive additions of further components to a given binding reaction over time. However, the relatively long dead time (10 s) in the original approach limited the transient-state kinetic analyses. The Duetta-Bio (Horiba) can be equipped with a SFA-20 stopped-flow rapid kinetics accessory (Horiba) that decreases the dead time to less than 8 ms, permitting the study of fast kinetic reactions (in the ms timescale) between two mixed reagents. Below, we detail the original approach from our recent study and discuss adaptations that utilize the SFA-20 stopped-flow rapid kinetics accessory (Horiba).

3. Equipment, materials & reagents

3.1 Equipment and software

Micropipettors.

Micropipettor tips.

A fluorescence spectrophotometer equipped with a temperature controller and capable of simultaneously detecting fluorescence emission intensities at two wavelengths. We use a Duetta-Bio (Horiba) equipped with EzSpec™ software. This device currently has the fastest spectral acquisition rate (510,000 nM/min) of any fluorescence spectrophotometer and can monitor fluorescence emission intensities at the peak emission intensity wavelengths for Cy3 (563 nM, I_{563}) and Cy5 (665 nM, I_{665}) essentially simultaneously ($\Delta t_I = 0.118$ ms), capturing data points every 0.17 s. For reactions with rate constants ≤ ~900/s, I_{563} and I_{665} change by ≤10% over the time interval of $\Delta t_I = 0.118$ ms. Furthermore, the Duetta-Bio (Horiba) can be equipped with the SFA-20 stopped-flow rapid kinetics accessory (Horiba) to study fast kinetic reactions (in the ms timescale) between two mixed reactants. This will be discussed in further detail below. It is also noted that a three-syringe version of the SFA-20 stopped-flow rapid kinetics accessory (Horiba) is available to provide an option for double-mixing.

Alternative fluorescence spectrophotometers may be used. However, the different spectral acquisition rates and corresponding Δt_I values need to be carefully considered with respect to the kinetics of a given reaction. If Δt_I is on the same time scale as a given kinetic reaction, the fluorescence emission intensities of the Cy3 donor and Cy5 acceptor may significantly change within Δt_I, leading to errors in the calculated FRET values.

The original approaches described below are performed in smaller (60 μL) volumes in a 45 μL Sub-Micro Fluorometer Cell (Starna, 16.45 F-Q-3/Z15) but can be performed in larger (120 μL) volumes in a 100 μL Sub-Micro Fluorometer Cell (Starna, 16.100 F-Q-10/Z15) by adjusting the concentrations and volumes of the added components. For all original approaches described below, solutions initially placed into the Fluorometer cell for recording fluorescence emission intensities should overfill the cell volume by at least 15% to raise the meniscus above the window aperture. After each experimental assay is completed, the fluorometer cell should be cleaned and dried prior to subsequent usage. Specifically, the contents of the fluorometer cell should be emptied, the cell incubated in a warm water/detergent solution, rinsed with a dilute acid, rinsed with copious volumes of water, and then dried.

All data described below is plotted and analyzed using Kaleidagraph from Synergy Software.

3.2 Materials required

Neutravidin (Thermo Scientific, PI131000.

Dithiothreitol (DTT) (GoldBio, I2481).

Ethylenediaminetetraacetic acid disodium salt dihydrate, EDTA•2Na•2 H_2O (BDH Chemicals, BDH4616)).

Glacial acetic acid (BDH Chemicals, BDH3094).

Glycerol (EMD Millipore, EMGX0185).

HEPES sodium salt (Fisher Bioreagents, BP410).

Hydrochloric acid, HCl (BDH Chemicals, BDH3028).

Potassium chloride, KCl (VWR Life Science, 0395).

Sodium chloride, NaCl (Supelco, SX0420).

Sodium hydroxide, NaOH (Thermo Scientific, 42,433–50,00).

Potassium hydroxide, KOH (BDH Chemicals, BDH9262).

Tris (VWR, 0826).

Adenosine 5′-O-(3-thio) triphosphate, ATPγS (Roche, 11162306001).

Adenosine triphosphate disodrium salt hydrate, ATP (Sigma, A3377).

Potassium acetate, KOAc (Alfa Aesar, 13449).

Magnesium acetate Tetrahydrate, $Mg(OAc)_2$•4 H_2O (Alfa Aesar, 36358).

Magnesium chloride Hexahydrate, $MgCl_2 \cdot 6H_2O$ (Alfa Aesar, 12288).

Calcium chloride anhydrous, $CaCl_2$ (Fisher Scientific, C614).

3.3 Buffers and solutions

1X TE buffer: 10 mM Tris, pH 8.0, 1 mM EDTA.

1X Annealing buffer: 10 mM TrisHCl, pH 8.0, 100 mM NaCl, 1 mM EDTA.

This buffer is first made as a 10X stock solution in which the pH is adjusted to pH 8.0 via addition of HCl and/or NaOH. For DNA annealing reactions, appropriate volumes of the 10X stock are added to the reaction mixture such that a 1X final concentration of the Annealing Buffer is achieved in the final reaction volume.

1X Mg^{2+} buffer: 25 mM HEPES, pH 7.5, 125 mM KOAc, 10 mM $Mg(OAc)_2$.

This buffer is first made as a 10X stock solution in which the pH is adjusted to pH 8.0 via addition of acetic acid and/or KOH. For assays, appropriate volumes of the 10X stock are added to the assay mixtures such that a 1X final concentration of the Mg^{2+} Buffer is achieved in the final assay volume.

1X Mg^{2+}/Ca^{2+} buffer: 20 mM HEPES, pH 7.5, 150 mM KCl, 5 mM $MgCl_2$, 5 mM $CaCl_2$.

This buffer is first made as a 10X stock solution in which the pH is adjusted to pH 8.0 via addition of HCl and/or KOH. For assays, appropriate volumes of the 10X stock are added to the assay mixtures such that a 1X final concentration of the Mg^{2+}/Ca^{2+} is achieved in the final assay volume.

Neutravidin buffer: 25 mM TrisHCl, pH 8.0, 120 mM NaCl, 20% glycerol (v/v).

500 mM KCl (in H_2O).

1M KOAc (in H_2O).

100 mM DTT (in H_2O, made fresh for each triplicate experiment).

100 μ**M Neutravidin** (in Neutravidin Buffer).

20% Glycerol (v/v, in H_2O).

3.4 The Cy3 donor/Cy5 acceptor FRET pair

A Cy3-labeled P/T DNA substrate (Fig. 3A–B, Cy3-P/T DNA) is utilized as the FRET donor in the approaches described below. The P/T DNA substrate is comprised of an unmodified template strand (62-mer) annealed to a 29-mer primer strand that contains the following modifications: a biotin at the 5′ terminus, a Cy3 donor 4 nt from the 5′ terminus (within the phosphodiester backbone) and a dideoxycytidine (ddC) at the 3′ terminus. Each constituent oligonucleotide comprising the P/T DNA substrate (i.e., template and primer strands) can be commercially synthesized by Integrated DNA Technologies (IDT,

Coralville, IA). Currently, a 3′ ddC is the only 3′ dideoxynucleotide modification offered by IDT. We purify each via denaturing polyacrylamide gel electrophoresis (PAGE) in the lab, resuspend in 1X TE Buffer (10 mM Tris, pH 8.0, 1 mM EDTA), and store at −20 °C. The concentrations of the unlabeled template strand is determined from its absorbance at 260 nM using the provided extinction coefficient (ε_{260} = 624,900/M/cm). The concentration of the primer strand is determined from its absorbance at 260 nm using the provided extinction coefficient (ε_{260} = 267,200/M/cm), which accounts for the Cy3-label, and from its absorbance at 550 nm using the extinction coefficient of Cy3 (ε_{550} = 136,000/M/cm). The Cy3-labeling efficiency for the primer (in %) is determined according to Eq. (1) below where $[DNA]_{260}$ and $[DNA]_{550}$ are the concentrations of the primer determined from its absorbance at 260 nm (using ε_{260}) and 550 nm (using ε_{550}), respectively. The labeling efficiency of PAGE purified primer strands is consistently >98%.

$$Cy3\ \ Labeling\ \ Efficiency = \frac{[DNA]_{550}}{[DNA]_{260}} \times 100\,\% \tag{1}$$

For annealing the P/T DNA substrate, the primer and template strands are mixed in equimolar amounts in 1X annealing buffer (10 mM TrisHCl, pH 8.0, 100 mM NaCl, 1 mM EDTA), heated to 95 °C for 5 min, and allowed to slowly cool to room temperature.

Cy5-labeled PCNA (Fig. 3C, Cy5-PCNA) is utilized as the FRET acceptor in the approaches described below. Specifically, C-terminal His_6-tagged, mutant human PCNA (C27M/C62M/C81S/C135S/C148S/C162S/N107C) is purified, labeled with Cy5 at amino acid position 107, and characterized as previously described (Hedglin & Perumal et al., 2013; Perumal et al., 2019). This amino acid position is located on the outer rim of the “back face” of the PCNA homotrimer at the subunit interfaces. The PCNA monomer Cy5-labeling efficiency is consistently between 30% and 40%, indicating that each PCNA homotrimer has ~ 1 one labeled monomer on average (as depicted in Fig. 3C). Neither the mutations nor the labeling of PCNA with Cy5 have any effect on its ability to interact with human RFC (Hedglin & Perumal et al., 2013).

The length (29 bp) of the dsDNA region within the annealed Cy3-P/T DNA substrate is in agreement with the requirements for assembly of a PCNA ring onto DNA by RFC (Hedglin et al., 2017; Hedglin & Benkovic, 2017b; Hedglin & Perumal et al., 2013). The ssDNA region adjacent to the 3′ hydroxyl terminus of the P/T junction is 33 nt in length and accommodates 1 RPA heterotrimer at the RPA:DNA ratios utilized in the approaches described below (Hoitsma et al., 2023; Kim et al., 1994; Kim et al., 1992; Kim & Wold, 1995). RPA engaged to the ssDNA region stabilizes loaded Cy5-PCNA at/near the P/T junction by prohibiting RFC-catalyzed unloading of Cy5-PCNA and diffusion of Cy5-PCNA along the adjacent ssDNA (Hedglin & Benkovic, 2017b). When pre-bound to neutravidin, the biotin attached to the 5′-end of the primer strand prevents loaded PCNA from sliding off the dsDNA end of the P/T DNA substrate, mimicking the aforementioned “protein roadblocks” (Hedglin & Benkovic, 2017b). The primer strand cannot be extended by a DNA polymerase due to the lack of a 3′ hydroxyl group. When Cy5-PCNA is encircling the

Cy3-P/T DNA substrate, the Cy3 donor and Cy5 acceptor are oriented towards each other, yielding FRET (Fig. 3D) (Hedglin & Perumal et al., 2013).

3.5 Other recombinant human proteins utilized

Wild-type, untagged human RPA is obtained as previously described (Nguyen et al., 2014). The concentration of active RPA was determined via a FRET-based activity assay as described previously (Li et al., 2020).

A truncated form of human RFC (hRFCp140Δ555) is obtained as previously described (Hedglin & Perumal et al., 2013; Perumal et al., 2019). In hRFCp140ΔN555, the N-terminal 555 amino acids of the large RFC subunit (i.e., RFC1, p140) is deleted to remove the nonspecific DNA-binding affinity of RFC. This region of the human clamp loader is conserved among eukaryotes and is dispensable for PCNA loading (Gomes et al., 2000; Podust et al., 1998; Uhlmann et al., 1997). Herein, the truncated form of human RFC is referred to as RFC. The concentration of RFC is determined via colorimetric Bradford Assay using Coomassie Blue G-250 dye and BSA as a standard.

Exonuclease-deficient, untagged, four-subunit human DNA pol δ is obtained as previously described (Hedglin & Perumal et al., 2013). The concentration of the four-subunit DNA pol δ complex is expressed as the concentration of the catalytic (POLD1, p125) subunit. This is determined by a published protocol (Hedglin et al., 2016). In short, purified four-subunit DNA pol δ complexes are separated on 10% denaturing SDS/PAGE together with known amounts of BSA to generate standard curves after Coomassie blue staining and densitometry of the gels. Digital images of the stained gels are analyzed with Image Lab 4.0 software (Bio-Rad). Herein, exonuclease-deficient, four-subunit human DNA pol δ is referred to as polδ.

4. Settings for the duetta-bio (Horiba) fluorescence spectrophotometer

Excitation and emission slit widths are 10 nm.

Excitation wavelength at 514 nm.

Emission wavelengths at 563 nm (peak fluorescence emission intensity wavelength of Cy3) and 665 nm (peak fluorescence emission intensity wavelength of Cy5).

The approaches described below are carried out in kinetics mode to record the fluorescence emission intensities (I) at the peak emission intensity wavelengths for Cy3 (563 nM, I_{563}) and Cy5 (665 nM, I_{665}) essentially simultaneously ($\Delta t = 0.118$ ms) over time. In the original approaches described below, once the recording is initiated by hand, the first recording occurs at 0.02 s and subsequent recordings occur every 0.17 s. In the new approaches described below, once mixing of the reactants is initiated, advancement of the stopped-syringe initiates the first recordings at < 8 ms.

5. Ionic strength conditions for assays

The interactions of DNA-binding proteins/protein complexes with DNA are central to the direct, ensemble FRET approaches described below. These and all protein•nucleic acid interactions are dependent on the ionic strength of the assay environment (Yu et al., 2020).[5] The ionic strength (I) of a solution is a measure of the concentration of all ions present in that solution (typically in mM) and is calculated according to Eq. (2) below where c_i is the molar concentration of ion i (in mM), z_i is the charge number of ion i, and the sum is taken over all ions in solution.[6]

$$I = \frac{1}{2}\sum_{i=1}^{n} c_i z_i^2 \tag{2}$$

All assays described below are carried out at physiological ionic strength (200 mM) for the final assay volume. The ionic strength of the final assay volume is adjusted to 200 mM by addition of appropriate amounts of either potassium acetate (KOAc) or potassium chloride (KCl) depending on the assay buffer (discussed further below). A significant deviation of the ionic strength from 200 mM may, and likely does, impact the transient state kinetics for the assays described below.

6. Buffer conditions for assays

The assays described below may be performed in either 1X Mg^{2+} buffer or 1X Mg^{2+}/Ca^{2+} buffer (described above), each supplemented with 1 mM DTT. At 200 mM ionic strength for the final assay volume, the presence of Ca^{2+} in the assay buffer does not affect the amount of RPA that binds to ssDNA nor the amount of PCNA encircling DNA, either as loaded PCNA (discussed further below) or as part of an activated loading complex (Norris et al., 2024). Ca^{2+} does affect the transient state kinetics observed for certain reactions (discussed further below). For assays performed in 1X Mg^{2+} buffer, the ionic strength of the final assay volume is adjusted to physiological (i.e., 200 mM) by addition of appropriate amounts of KOAc. For assays performed in 1X Mg^{2+}/Ca^{2+} buffer, the ionic strength of the final assay volume is adjusted to 200 mM by the addition of appropriate amounts of KCl.

7. Dilution of protein/protein complex stocks for use in assays

The stock concentrations of NeutraAvidin and all recombinant human protein/protein complexes described above are typically too high for direct use in the assays described below. Therefore, each of these proteins are diluted into pre-chilled 1X buffer (either 1X Mg^{2+} buffer or 1X Mg^{2+}/Ca^{2+} buffer) supplemented with 1 mM DTT and the ionic strength adjusted to 200 mM with appropriate amounts of a respective salt (either KOAc or KCl). For

[5]For more details on the biophysical principles underlying the ionic strength-dependence of nucleic acid-binding protein•nucleic interactions, readers are directed to one of the many excellent reviews in the literature, such as cited references.

[6]For assay solutions containing molecules, such as EDTA, with multiple ionizable groups, the concentration of all ionized species of the given molecule must be accounted for in the calculation of the ionic strength.

dilutions of RFC, the buffer is also supplemented with ATP or ATPγS. For dilutions of RFC into 1X Mg^{2+}/Ca^{2+} buffer, the buffer must also be supplemented with 10% glycerol (v/v). All diluted stocks are stored on ice until use and are stable for at least 5 min.

8. Direct, ensemble FRET approaches to monitor binding and activation of loading complexes at P/T junctions

During PCNA loading, RFC, with bound ATP, engages the "front face" of a free PCNA, opens the clamp, and the resultant complex, referred to herein as the loading complex, engages a P/T junction such that the "front face" of PCNA is oriented towards the 3′ terminus of the primer (Hedglin & Kumar et al., 2013). Upon engaging a P/T junction, the loading complex adopts an activated conformation in which ATP hydrolysis by RFC is optimized (Fig. 2A, *Step 1*). Herein, the activated conformation of the loading complex is referred to as the activated loading complex. Binding and activation of loading complexes can be monitored using intermolecular FRET between the Cy3 donor near the dsDNA end of the Cy3-P/T DNA substrate and the Cy5 acceptor on the outer rim of the "back face" of Cy5-PCNA, as illustrated in Fig. 4A (Hedglin & Benkovic, 2017b; Norris et al., 2024). To do so, a hydrolysis-resistant ATP analog is required to stall the PCNA loading pathways at activation of the loading complex. We utilize adenosine 5′-O-(3-thio) triphosphate (ATPγS) where one of the non-bridging oxygens of the γ-phosphoryl group is substituted for sulfur, severely inhibiting ATP hydrolysis by human RFC (Hedglin & Perumal et al., 2013; Kang et al., 2019). Other ATP analogs that also mimic the "pre-hydrolytic" state of ATP hydrolysis when bound by a protein may also be utilized. For example, adenylyl imidodiphosphate (AMPPNP), adenylyl methylenediphosphate (AMPPCP), alpha,beta-methylene-triphosphonate (AMPCPP), and ADP-beriylium fluoride (ADP-BeF_X). Use of ATP analogs that mimic the transition state of ATP hydrolysis when bound by a protein, such as ADP-aluminum fluoride (ADP:AlF_x), ADP-magnesium fluoride (ADP:MgF_x), and ADP-vanidate (ADP:V_i) may lead to additional phases in the transitions from low to high FRET states (Lacabanne et al., 2020).

The original approach described in Fig. 4A is performed in 1X Mg^{2+}/Ca^{2+} buffer (supplemented with 1 mM DTT) under conditions where the final concentrations of each reaction component (after final mixing) was as follows; 20 nM Cy3-P/T DNA substrate, 80 nM NeutrAvidin (homotetramer), 1 mM ATPγS, 25 nM RPA (heterotrimer), 20 nM Cy5-PCNA (homotrimer), 20 nM RFC (heteropentamer). Upon addition of loading complexes preformed with ATPγS and Cy5-PCNA, I_{665} instantly increases concomitantly with an instant decrease in I_{563} after which I_{665} continues to increase slowly while I_{563} continues to decrease slowly (Fig. 4B, *Top*). These synchronized, anti-correlated changes in I_{563} and I_{665} are indicative of the appearance and increase FRET. Thus, binding and activation of loading complexes preformed with ATPγS and Cy5-PCNA results in a multi-phase transition from a low FRET (~0.12) to a high FRET (>0.35) state (Fig. 4B, *Bottom*). Specifically, loading complexes rapidly engage all P/T junctions, slowly adopt activated conformations, and then the PCNA loading pathways stall prior to ATP hydrolysis (Hedglin & Benkovic, 2017b; Hedglin & Perumal et al., 2013; Kang et al., 2019; Waga & Stillman, 1998). Initial binding of loading complexes to P/T junctions occurs with an extremely fast rate constant

$\left(k_{\text{inc 1}} = 1.98 \times 10^8/\text{M/s} - 2.63 \times 10^8/\text{M/s}\right)$. In the original approach, this initial phase occurs within the dead time of the assay and, hence, it's observed rate constant ($k_{\text{obs inc 1}}$) cannot be determined (discussed further below) (Hedglin & Benkovic, 2017b). Following initial binding, adoption of the activated conformations of loading complexes is biphasic. To determine the amplitudes ($A_{\text{inc 2}}$ and $A_{\text{inc 3}}$) and rate constants ($k_{\text{obs inc 2}}$, $k_{\text{obs inc 3}}$) for each of these phases, the FRET values observed after the addition of loading complexes pre-formed with ATPγS and Cy5-PCNA are fit to a double-exponential kinetic rate equation that also accounts for the amplitude of the initial phase ($A_{\text{inc 1}}$) that occurs within the dead time.

8.1 Original approach to monitor binding and activation of loading complexes experimental assay (Fig. 4A)

1. Make a 60 μL solution (Solution A) containing 22.2 nM Cy3-P/T DNA P/T DNA, 88.9 nM NeutrAvidin (homotetramer), 1 mM ATPγS, and 27 nM RPA (heterotrimer) in 1X Mg^{2+}/Ca^{2+} Buffer (see Buffers and solutions) supplemented with 1 mM DTT and ionic strength adjusted to 200 mM by addition of appropriate volume of 500 mM KCl. Store Solution A at room temperature.
2. Make a 10 μL solution (Solution B) containing 200 nM Cy5-PCNA (homotrimer), 200 nM RFC (heteropentamer), and 1 mM ATPγS in 1X Mg^{2+}/Ca^{2+} Buffer (see Buffers and solutions) supplemented with 1 mM DTT and ionic strength adjusted to 200 mM by addition of appropriate volume of 500 mM KCl. Store solution B on ice.
3. Transfer Solution A to the fluorometer cell and place the cell in the instrument. Record I_{563} and I_{665} until both stabilize for at least 1 min (i.e. reach equilibrium).
4. After I_{563} and I_{665} have stabilized for at least one minute, pause the recording, add 6.68 μL of Solution B to the cell, avidly mix the resultant solution via pipetting, and then record I_{563} and I_{665}, taking note of the time between the addition of Solution B and the resumption of the recording (i.e., the dead time). The volume of Solution B (6.68 μL) added to Solution A in the cell (60 μL) is 10% of the final reaction volume (66.68 μL). This volume ensures rapid and thorough mixing without changing the temperature of the final reaction solution.

Control assays—Solution A in the experimental assays described above lacks the Cy5 acceptor (Cy5-PCNA). Thus, I_{563} and I_{665} values recorded for Solution A only (i.e., prior to the addition of Solution B) and their corresponding FRET values do not represent a true experimental baseline. To determine the experimental baseline, control assays must be performed, and the data analyzed as described below.

1. Make a 60 μL solution containing 20 nM Cy3-P/T DNA P/T DNA, 80 nM NeutrAvidin (homotetramer), 1 mM ATPγS, and 25 nM RPA (heterotrimer) in 1X Mg^{2+}/Ca^{2+} Buffer (see Buffers and solutions) supplemented with 1 mM DTT and ionic strength adjusted to 200 mM by addition of appropriate volume of 500 mM KCl. Transfer the solution to the fluorometer cell and place the cell in the

instrument. Record I_{563} and I_{665} until both stabilize for at least 1 min (i.e. reach equilibrium).

2. Make a 60 μL solution containing 20 nM Cy5-PCNA (homotrimer), 20 nM RFC (heteropentamer), and 1 mM ATPγS in 1X Mg^{2+}/Ca^{2+} Buffer (see Buffers and solutions) supplemented with 1 mM DTT and ionic strength adjusted to 200 mM by addition of appropriate volume of 500 mM KCl. Transfer the solution to the fluorometer cell and place the cell in the instrument. Record I_{563} and I_{665} until both stabilize for at least 1 min (i.e. reach equilibrium).

3. Data analysis: I_{563} and I_{665} time trajectories from experimental assays (Fig. 4B, *Top*) assays (Fig. 4B, *Top*)

4. Extract I_{563} and I_{665} values observed for Solution A at equilibrium over the final minute of recording in step 8.1.3. above. Plot these values as a function of time, from 0.02 to 60.03 s

5. Extract I_{563} and I_{665} values observed after the addition of Solution B in step 8.1.4 above and multiply each value by a dilution factor according to Eq. (3) below where V_A is volume of Solution A in the cell and V_B is the volume of Solution B added to Solution A in the cell.

$$Dilution\ \ Factor = \frac{V_A + V_B}{V_A} \tag{3}$$

Under these conditions the dilution factor is equal to $\frac{60uL + 6.68uL}{60uL} = 1.11$.

6. On the same graph from 8.1.7., plot the corrected I_{563} and I_{665} values from 8.1.8 above as a function of time, beginning at 60.03 s and adjusting for the dead time.

7. Inspect the time trajectories of the I_{563} and I_{665}. The appearance and increase in FRET is only confirmed by synchronized and anti-correlated changes in the time trajectories of I_{563} and I_{665} observed upon addition of Solution B to Solution A in the cell. Specifically, I_{563} decreases simultaneously with increases in I_{665}.

   Data analysis: E_{FRET} time trajectories (Fig. 4B, *Bottom*)

   For I_{665} and I_{563} values recorded at time t during an experimental assay (8.1.1–8.1.4), the approximate FRET efficiency ($E^{Exp}_{FRET,t}$) is calculated from Eq. (4) below where $I^{Exp}_{563,t}$ and $I^{Exx}_{665,t}$ represent the I_{563} and I_{665} values recorded during an experimental assay at time t, respectively.

$$E^{Exp}_{FRET,t} = \frac{I^{Exp}_{665,t}}{I^{Exp}_{665,t} + I^{Exp}_{563,t}} \tag{4}$$

For I_{665} and I_{563} values recorded at time t during control assays (8.1.5–8.1.6), the approximate FRET efficiency $\left(E_{FRET,t}^{Con}\right)$ is calculated from Eq. (5) below where $I_{563,t}^{DNA}$ and $I_{665,t}^{DNA}$ represent the I_{563} and I_{665} values recorded at time t, respectively, for a control assay lacking only the Cy5-PCNA loading complex (8.1.5.). $I_{563,t}^{Loading\ Complex}$ and $I_{665,t}^{Loading\ Complex}$ represent the I_{563} and I_{665} values recorded at time t, respectively, for a control assay containing only the Cy5-PCNA loading complex (8.1.6).

$$E_{FRET,t}^{Con} = \frac{\left(I_{665,t}^{Loading\ Complex} + I_{665,t}^{DNA}\right)}{\left(I_{665,t}^{Loading\ Complex} + I_{665,t}^{DNA}\right) + \left(I_{563,t}^{Loading\ Complex} + I_{563,t}^{DNA}\right)} \quad (5)$$

8. Calculate $E_{FRET,t}^{Exp}$ from I_{563} and I_{665} values from 8.1.7 above according to Eq. (4) and plot these values as a function of time, from 0.02 to 60.03 s

9. Extract I_{563} and I_{665} values observed at equilibrium over the final minute of the recordings in 8.1.5. and 8.1.6. above and calculate $E_{FRET,t}^{Con}$ according to Eq. (5). On the same graph from 8.1.11 above, plot these values as a function of time, from 60.03 to 120.04 s. The time trajectory of this E_{FRET} represents the predicted E_{FRET} trace for no interaction between Cy3-P/T DNA•RPA complexes and the Cy5-PCNA loading complexes (pink trace in Fig. 4B, *Bottom*). Fitting this data to a flat line yields the E_{FRET} value for the low FRET state, $E_{FRET}^{Low}\left(E_{FRET}^{Low} = 0.121 \pm 2.13 \times 10^{-4}/\text{s}\right.$ for Fig. 4B, *Bottom*).

10. Calculate $E_{FRET,t}^{Exp}$ from I_{563} and I_{665} values from 8.1.8 above according to Eq. (4). On the same graph from 8.1.11. above, plot these values as a function of time, beginning at 60.03 s, adjusting for the dead time. E_{FRET} values observed after the addition of Solution B to Solution A in the cell (i.e., after but not including 60.03 s) are fit to Eq. (6) below where $E_{FRET,i}$ is the extrapolated E_{FRET} value at 60.03 s and is equal to the sum of E_{FRET}^{Low} (described above) and $A_{inc\ 1}\left(E_{FRET,i} = A_{inc\ 1} + E_{FRET}^{Low}\right)$.

$$E_{FRET,t} = E_{FRET,i} + A_{inc2}\left(1 - e^{(t - 60.03s)k_{obs\ inc2}}\right) + A_{inc3}\left(1 - e^{(t - 60.03s)k_{obs\ inc3}}\right) \quad (6)$$

$A_{inc\ 1}$ is calculated by subtracting E_{FRET}^{Low} from $E_{FRET,i}(A_{inc\ 1} = 0.104 \pm 0.012$ for Fig. 4B, *Bottom*).

Summing the calculated values for $E_{FRET,i}$, $A_{inc\ 2}$, and $A_{inc\ 3}$ from the kinetic fit yields the E_{FRET} value for the high FRET state, $E_{FRET}^{High}\left(E_{FRET}^{High} = 0.484 \pm 0.018\right.$ for Fig. 4B, *Bottom*).

8.2 New approach to monitor binding and activation of loading complexes

In the original approach described above (8.1., Fig. 4A), the initial phase of the FRET increase occurs within the dead time of the assay (≤10 s) and, hence, it's observed rate

constant ($k_{obs\ inc\ 1}$) cannot be determined. To monitor the initial phase of the FRET increase, as well as any reaction with fast kinetics (in the ms timescale), the Duetta-Bio can be equipped with an SFA-20 stopped-flow rapid kinetics accessory (Horiba). This accessory was designed and optimized for SPEX® instruments, such as FluoroMax® and FluoroLog®, but can be utilized with the Duetta-Bio. The accessory is connected to the Duetta-Bio via a BNC connector cable. In the conventional two-syringe mixing system, the reactant solutions are contained in separate drive syringes that are mounted on a rigid-drive platform. Under pneumatic drive activation, the pistons of the drive syringes are simultaneously driven, forcing the two reactants through a mixing chamber. The result mixtures passes through to a fluorometer cell within the Duetta-Bio and into a stopped syringe. Advancement of the stopped syringe by the mixed reactants triggers data acquisition by the Duetta-Bio. The time interval between mixing of the reagent solutions in the mixing chamber and the beginning of the fluorescence intensities recordings in the fluorometer cell (i.e., dead time) is < 8 ms. In this approach, the minimum volume per reactant per determination is 100 μL. Below, we detail a new approach (based on 100 μL reactant volumes and a 1:1 mixing ratio) to monitor the complete reaction for binding and activation of loading complexes (Fig. 5). The reactant volumes can be adjusted accordingly for the desired number of replicate determinations.

Experimental assay (Fig. 5)

1. Make a 100 μL solution (Solution A) containing 40 nM Cy3-P/T DNA P/T DNA, 160 nM NeutrAvidin (homotetramer), 1 mM ATPγS, and 50 nM RPA (heterotrimer) in 1X Mg^{2+}/Ca^{2+} Buffer (see Buffers and solutions) supplemented with 1 mM DTT and ionic strength adjusted to 200 mM by addition of appropriate volume of 500 mM KCl. Store Solution A at room temperature.
2. Make a 100 μL solution (Solution B) containing 40 nM Cy5-PCNA (homotrimer), 40 nM RFC (heteropentamer), and 1 mM ATPγS in 1X Mg^{2+}/Ca^{2+} Buffer (see Buffers and solutions) supplemented with 1 mM DTT and ionic strength adjusted to 200 mM by addition of appropriate volume of 500 mM KCl. Store solution B on ice.
3. Transfer Solution A to Syringe A and Solution B to Syringe B.
4. Turn on the trigger in command. Start the acquisition, recording I_{563} and I_{665}.

Data analysis

5. Plot the recorded I_{563} and I_{665} values as a function of time and inspect the time trajectories. The appearance and increase in FRET is only confirmed by synchronized and anti-correlated changes in the time trajectories of I_{563} and I_{665} observed upon mixing of Syringe A with Syringe B. Specifically, I_{563} decreases simultaneously with increases in I_{665}.
6. Calculate $E_{FRET,t}^{Exp}$ from I_{563} and I_{665} values from 8.2.4 above according to Eq. (4) and plot these values as a function of time. Fit the $E_{FRET,t}^{Exp}$ values to Eq. (7) below.

$$E_{FRET,t} = A_{inc1}\left(1 - e^{(t \times k_{2bs\ inc1})}\right) + A_{inc2}\left(1 - e^{(t \times k_{0bs\ inc2})}\right) + A_{inc3}\left(1 - e^{(t \times k_{0bs\ inc3})}\right) \quad (7)$$

9. Direct, ensemble FRET assay to monitor the rate-limiting step of PCNA loading

ATP hydrolysis by RFC within an activated loading complex simultaneously closes PCNA around a nascent P/T junction and releases the closed (i.e., loaded) PCNA onto the upstream dsDNA region. The resultant RFC•ADP complex then releases into solution via dissociation from the resident RPA, permitting loaded PCNA to simultaneously reposition on the dsDNA region of the P/T junction (Fig. 2A, Step 3) (Hedglin & Benkovic, 2017b; Hedglin & Kumar et al., 2013; Hedglin & Perumal et al., 2013; Yuzhakov et al., 1999). Release of RFC•ADP complexes and the simultaneous repositioning of loaded PCNA is the rate-limiting step of the PCNA loading pathway and this step can be monitored using intermolecular FRET between the Cy3 donor near the dsDNA end of the Cy3-P/T DNA substrate and the Cy5 acceptor on the outer rim of the “back face” of Cy5-PCNA, as illustrated in Fig. 6A (Hedglin & Benkovic, 2017b; Norris et al., 2024).

The approach described in Fig. 6A is performed in 1X Mg^{2+}/Ca^{2+} buffer (supplemented with 1 mM DTT) under conditions where the final concentrations of each reaction component (after final mixing) was as follows; 20 nM Cy3-P/T DNA substrate, 80 nM NeutrAvidin (homotetramer), 1 mM ATP, 25 nM RPA (heterotrimer), 20 nM Cy5-PCNA (homotrimer), 20 nM RFC (heteropentamer). Upon addition of RFC • ATP complexes, I_{665} increases concomitantly with a decrease in I_{563} after which both I_{665} and I_{563} stabilize and persist over time (Fig. 6B, *Top*). These synchronized, anti-correlated changes in I_{563} and I_{665} are indicative of the appearance and increase FRET. Thus, RFC•ATP complexes binding “free” Cy5-PCNA in solution and subsequently loading Cy5-PCNA onto Cy3-P/T DNA substrates results in a multiphase transition from a low FRET (~0.16) to a high FRET (~0.53) state (Fig. 6B, *Bottom*). Specifically, Cy5-PCNA is first loaded onto all Cy3-P/T DNA substrates and this step is rate-limited by a kinetic step ($k_{\text{obs inc 1}}$) along the PCNA loading pathway that occurs prior to and much slower than binding of the loading complexes to P/T junctions (Fig. 2A, *Step 1*). Next, loaded PCNA reposition relatively slower ($k_{\text{obs inc 2)}}$ on the P/T junctions concurrent with release of RFC•ADP complexes into solution via their dissociation from the resident RPA (Hedglin & Benkovic, 2017b). To determine the amplitudes ($A_{\text{inc 1}}$ and $A_{\text{inc 2}}$) and rate constants ($k_{\text{obs inc 1}}$, $k_{\text{obs inc 2}}$) for each of the observed phases, the FRET values observed upon the addition of RFC•ATP complexes are fit to a double-exponential kinetic rate equation. It is noted that the rate constant of interest, $k_{\text{obs inc 2,}}$, is independent of the experimental buffer (either 1X Mg^{2+}/Ca^{2+} or 1X Mg^{2+}). $k_{\text{obs inc 1}}$ is ~2-fold slower in 1X Mg^{2+}/Ca^{2+} compared to that observed in 1X Mg^{2+} buffer (Norris et al., 2024).

9.1 Approach to monitor the rate-limiting step of PCNA loading

Experimental assay (Fig. 6A)

1. Make a 60 μL solution (Solution A) containing 22.2 nM Cy3-P/T DNA P/T DNA, 88.9 nM NeutrAvidin (homotetramer), 1 mM ATP, 27 nM RPA (heterotrimer), and 22.2 nM Cy5-PCNA (homotrimer) in 1X Mg^{2+}/Ca^{2+} Buffer (see Buffers and solutions) supplemented with 1 mM DTT and ionic strength adjusted to 200 mM by addition of appropriate volume of 500 mM KCl. Cy5-PCNA must be added last to the solution mixture to eliminate any possibility of spontaneous (i.e., non-catalyzed) loading of Cy5-PCNA onto Cy3-P/T DNA substrates. Store Solution A at room temperature.

2. Make a 10 μL solution (Solution B) containing 200 nM RFC (heteropentamer) and 1 mM ATP in 1X Mg^{2+}/Ca^{2+} Buffer (see Buffers and solutions) supplemented with 1 mM DTT and ionic strength adjusted to 200 mM by addition of appropriate volume of 500 mM KCl. Store solution B on ice.

3. Transfer Solution A to the fluorometer cell and place the cell in the instrument. Record I_{563} and I_{665} until both stabilize for at least 1 min (i.e. reach equilibrium).

4. After I_{563} and I_{665} have stabilized for at least one minute, pause the recording, add 6.68 μL of Solution B to the cell, avidly mix the resultant solution via pipetting, and then record I_{563} and I_{665}, taking note of the time between the addition of Solution B and the resumption of the recording (i.e., the dead time). The volume of Solution B (6.68 μL) added to Solution A in the cell (60 μL) is 10% of the final reaction volume (66.68 μL). This volume ensures rapid and thorough mixing without changing the temperature of the final reaction solution.

   Data analysis: Time trajectories of I_{563} and I_{665} values from experimental assays (Fig. 6B, *Top*)

5. Extract I_{563} and I_{665} values observed for Solution A at equilibrium over the final minute of recording in step 9.1.3. above. Plot these values as a function of time, from 0.02 to 60.03 s. Because Solution A contains both the Cy3 donor (Cy3-P/T DNA) and Cy5 acceptor (Cy5-PCNA), the fluorescence intensity values recorded for Solution A only (i.e., prior to the addition of Solution B) and their corresponding FRET values represent a true experimental baseline.

6. Calculate the average of the I_{563} values and the average of the I_{665} values from step 9.1.5. above. These averages represent the I_{563} and I_{665} values observed prior to the addition of Solution B (at 60.03 s). Extract I_{563} and I_{665} values observed after the addition of Solution B in step 9.1.4. above and multiply each value by a dilution factor according to Eq. (3) above. Under these conditions the dilution factor is equal to $\frac{60uL + 6.68uL}{60uL} = 1.11$.

7. On the same graph from 9.1.5., plot all calculated and corrected I_{563} and I_{665} values from 9.1.6. above as a function of time, beginning at 60.03 s and adjusting for the dead time.

8. Inspect the time trajectories of the I_{563} and I_{665} values. The appearance and increase in FRET is only confirmed by synchronized and anticorrelated changes in the time trajectories of I_{563} and I_{665} observed upon addition of Solution B to Solution A in the cell. Specifically, I_{563} decreases simultaneously with increases in I_{665}.

Data analysis: E_{FRET} time trajectories (Fig. 6B, *Bottom*)

9. Calculate $E_{FRET,t}^{Exp}$ from I_{563} and I_{665} values from 9.1.5. above according to Eq. (4) and plot these values as a function of time, from 0.02 to 60.03 s. The time trajectory of this E_{FRET} represents the experimental E_{FRET} trace for no interaction between Cy3-P/T DNA•RPA complexes and Cy5-PCNA. Fitting this data to a flat line yields the E_{FRET} value for the low FRET state $\left(E_{FRET}^{Low} = 0.164 + 7.82 \times 10^{-5}\ \mathrm{s}^{-1}\right.$ for Fig. 6B, *Bottom*).

10. Calculate $E_{FRET,t}^{Exp}$ from I_{563} and I_{665} values from 9.1.6. above according to Eq. (4). On the same graph from 9.1.9. above, plot these values as a function of time, beginning at 60.03 s and adjusting for the dead time. E_{FRET} values observed upon the addition of Solution B to Solution A in the cell (i.e., after and including 60.03 s) are fit to Eq. (8) below where $E_{FRET,i}$ is the extrapolated E_{FRET} value at 60.03 s and should be equal to E_{FRET}^{Low} for this particular assay (described above).

$$E_{FRET,t} = E_{FRET,i} + A_{inc1}\left(1 - e^{(t - 60.03s)k_{obs\ inc1}}\right) + A_{inc2}\left(1 - e^{(t - 60.03s)k_{obs\ inc2}}\right) \quad (8)$$

Summing the calculated values for $E_{\mathrm{FRET},,i}$, $\mathrm{A}_{\mathrm{inc}\ 1}$, and $\mathrm{A}_{\mathrm{inc}\ 2}$ from the kinetic fit yields the E_{FRET} value for the high FRET state for this particular assay $\left(E_{FRET}^{High} = 0.530 \pm 0.002\right.$ for Fig. 6B, *Bottom*). $E_{FRET,i} = 0.189 \pm 0.001$ for Fig. 6B, which is within 15.3 ± 6.6% of E_{FRET}^{Low} for Fig. 6B, *Bottom* ($0.164 \pm 7.82 \times 10^{-5}\ \mathrm{s}^{-1}$). This indicates that the entire E_{FRET} time trajectory observed upon the addition of Solution B to Solution A in the cell, including the dead time, can be accurately fit to a double exponential rise to determine $k_{\mathrm{obs\ inc}\ 1}$ and $k_{\mathrm{obs\ inc}\ 2}$. The latter is the rate constant of interest.

10. Direct, ensemble FRET assay to monitor formation of pol δ holoenzymes and initiation of DNA synthesis

In the final steps of human pol δ holoenzyme assembly and initiation of DNA synthesis, pol δ engages the “front face” of loaded PCNA and the P/T junction, forming a holoenzyme (Fig. 2B, Step 1), and aligns an incoming, complimentary dNTP at the 3′ terminus of the primer strand to initiate DNA synthesis (Fig. 2B, *Step 2*). These steps can be monitored using intermolecular FRET between the Cy3 donor near the dsDNA end of the Cy3-P/T DNA substrate and the Cy5 acceptor on the outer rim of the “back face” of Cy5-PCNA, as illustrated in Fig. 7A (Norris et al., 2024). To do so, the following are required to stabilize the primer strand within the Cy3-P/T DNA substrate. First, exonuclease-deficient pol δ is

required to prevent degradation of the primer strand. We utilize an exonuclease-deficient human pol δ mutant that contains a single point mutation (D402A) within the exonuclease domain of the catalytic subunit (p125/POLD1). This conserved residue is critical for divalent metal binding and the D402A mutation completely abolishes exonuclease activity (Hedglin et al., 2016; Schmitt et al., 2009). Second, the primer strand of the Cy3-P/T DNA substrate must contain a dideoxynucleotide at its 3′ terminus to prevent primer extension. We utilize ddC as it is currently the only 3′ dideoxynucleotide modification offered by IDT. The complimentary template DNA sequence is designed such that ddC is correctly base-paired with a guanine (G).

The assays described in Fig. 7A were performed in 1X Mg^{2+}/Ca^{2+} buffer (supplemented with 1 mM DTT) under conditions where the final concentrations of each reaction component (after final mixing) was as follows; 20 nM Cy3-P/T DNA substrate, 80 nM NeutrAvidin (homotetramer), 1 mM ATP, 1 mM dGTP, 25 nM RPA (heterotrimer), 20 nM Cy5-PCNA (homotrimer), 20 nM RFC (heteropentamer), and 20 nM pol δ (hetertetramer). First, PCNA is loaded onto the Cy3-P/T DNA substrate (as described above and depicted in Fig. 6A), resulting in synchronized, anti-correlated changes in I_{563} and I_{665} (Fig. 7B, *Top*), indicative of a biphasic transition from a low FRET (~0.20) to a high FRET (~0.53) state (Fig. 7B, *Bottom*). Loaded PCNA rapidly and randomly diffuses along the dsDNA regions of P/T junctions (Hedglin & Benkovic, 2017b; Kochaniak et al., 2009) and these diffusive movements are kinetically invisible in the present assays. Thus, the high FRET state observed at the plateau of Cy5-PCNA loading (Fig. 7B, *Bottom*) reports on the average distance between loaded Cy5-PCNA and the 5′ terminus of the primer strand within the Cy3-P/T DNA substrate. Next, pol δ and dGTP are simultaneously added such that the final concentration of pol δ is at least stoichiometric to the concentrations of Cy3-P/T DNA and Cy5-PCNA (i.e., pol δ:Cy5 – PCNA:Cy3-P/T DNA = 1:1:1). Upon the simultaneous addition of pol δ and dGTP, I_{665} instantly increases further concomitantly with an instant, further decrease in I_{563} after which I_{665} continues to increase slowly while I_{563} continues to decrease slowly (Fig. 7B, *Top*). These synchronized, anti-correlated changes in I_{563} and I_{665} are indicative of a further increase in FRET and require both pol δ and the correct dNTP (Norris et al., 2024). Thus, formation of pol δ holoenzymes and adoption of the initiation state for DNA synthesis results in a multi-phase transition from a high FRET (~0.53) to a secondary high FRET (~0.70) state (Fig. 7B, *Bottom*). Specifically, pol δ rapidly engages the “front face” of loaded PCNA and the P/T junction (forming a holoenzyme) and aligns an incoming, complimentary dNTP at the 3′ terminus of the primer strand to initiate DNA synthesis. In the original approach, this initial phase occurs within the dead time of the assay and, hence, it’s observed rate constant ($k_{\text{obs inc 1}}$) cannot be determined (discussed further below) (Hedglin & Benkovic, 2017b). The next phase in the transition to the secondary high FRET state is observable. To determine the amplitude (A_{inc} 2) and observed rate constant ($k_{\text{obs inc 2}}$) for this second phase, the FRET values observed after the simultaneous addition of pol δ and dGTP are fit to a single-exponential rate equation that also accounts for the amplitude of the initial phase ($A_{\text{inc 1}}$) that occurs within the dead time.

Currently, it is unknown what the second phase in the transition to the secondary FRET state represents (Fig. 7B, *Bottom*). In a recent cryogenic electron microscopy (cryo-EM) study on

the initiation state of human pol δ holoenzymes, the orientations of the engaged PCNA in the various 3D classifications varied in range relative to the dsDNA regions of the P/T junctions by up to ~20°. Such tilting orients the outer rim of the engaged PCNA an additional ~ 30 Å A closer to 5′ terminus of the primer strand (Lancey et al., 2020). Thus, perhaps the second phase in the transition to the secondary FRET state (Fig. 7B, *Bottom*) reports on the engaged PCNA sampling various orientations as it approaches an equilibrium that reflects the average orientation. Future studies are required to substantiate or refute this hypothesis.

10.1 Original approach to monitor formation of pol δ holoenzymes and initiation of DNA synthesis

Experimental assay (Fig. 7A)

1. Make a 60 μL solution (Solution A) containing 24.7 nM Cy3-P/T DNA P/T DNA, 98.8 nM NeutrAvidin (homotetramer), 1.12 mM ATP, 30.9 nM RPA (heterotrimer), and 24.7 nM Cy5-PCNA (homotrimer) in 1X Mg^{2+}/Ca^{2+} Buffer (see Buffers and solutions) supplemented with 1 mM DTT and ionic strength adjusted to 200 mM by addition of appropriate volume of 500 mM KCl. Cy5-PCNA must be added last to the solution mixture to eliminate any possibility of spontaneous (i.e., non-catalyzed) loading of Cy5-PCNA onto Cy3-P/T DNA substrates. Store Solution A at room temperature.
2. Make a 10 μL solution (Solution B) containing 222 nM RFC (heteropentamer) and 1.12 mM ATP in 1X Mg^{2+}/Ca^{2+} Buffer (see Buffers and solutions) supplemented with 1 mM DTT and ionic strength adjusted to 200 mM by addition of appropriate volume of 500 mM KCl. Store solution B on ice.
3. Make a 10 μL solution (Solution C) containing 200 nM pol δ (heterotetramer) and 10 mM dGTP in 1X Mg^{2+}/Ca^{2+} Buffer (see Buffers and solutions) supplemented with 1 mM DTT and ionic strength adjusted to 200 mM by addition of appropriate volume of 500 mM KCl. Store solution C on ice.
4. Transfer Solution A to the fluorometer cell and place the cell in the instrument. Record I_{563} and I_{665} until both stabilize for at least 1 min (i.e. reach equilibrium).
5. After I_{563} and I_{665} have stabilized for at least one minute, pause the recording, add 6.68 μL of Solution B to the cell, avidly mix the resultant solution via pipetting, and then record I_{563} and I_{665}, taking note of the time between the addition of Solution B and the resumption of the recording (i.e., the dead time). The volume of Solution B (6.68 μL) added to Solution A in the cell (60 μL) is 10% of the total reaction volume (66.68 μL) after the addition of Solution B. This volume ensures rapid and thorough mixing without changing the temperature of the final reaction solution.
6. After I_{563} and I_{665} have stabilized for at least one minute, pause the recording, add 7.42 μL of Solution C to the cell, avidly mix the resultant solution via pipetting, and then record I_{563} and I_{665}, taking note of the time between the addition of Solution C and the resumption of the recording (i.e., the dead time).

Dead times ≤10 s. The volume of Solution B (7.42 μL) added to the mixed volume in the cell (60 μL Solution A+6.68 μL Solution B = 66.68) is 10% of the final reaction volume (74.1 μL). This volume ensures rapid and thorough mixing without changing the temperature of the final reaction solution.

Data analysis: Time trajectories of I_{563} and I_{665} values from experimental assays (Fig. 7B, *Top*)

7. Extract I_{563} and I_{665} values observed for Solution A at equilibrium over the final minute of recording in step 10.1.4. above. Plot these values as a function of time, from 0.02 to 60.03 s. Because Solution A contains both the Cy3 donor (Cy3-P/T DNA) and Cy5 acceptor (Cy5-PCNA), the fluorescence intensity values recorded for Solution A only (i.e., prior to the addition of Solution B) and their corresponding FRET values represent a true experimental baseline.

8. Calculate the average of the I_{563} values and the average of the I_{665} values from step 10.1.7. above. These averages represent the I_{563} and I_{665} values observed prior to the addition of Solution B (at 60.03 s). Extract I_{563} and I_{665} values observed after the addition of Solution B in step 10.1.5. above and multiply each value by a dilution factor according to Eq. (3) above. Under these conditions the dilution factor is equal to $\frac{60uL + 6.68uL}{60uL} = 1.11$.

9. On the same graph from 10.1.7., plot all calculated and corrected I_{563} and I_{665} values from 10.1.8. above as a function of time, beginning at 60.03 s and adjusting for the dead time.

10. Calculate the average of the corrected I_{563} values and the average of the corrected I_{665} values observed over the final 60 s of the traces above in 10.1.9. These averages represent the I_{563} and I_{665} values observed prior to the addition of Solution C (at 410.05 s). Extract I_{563} and I_{665} values observed after the addition of Solution C in step 10.1.6. above and multiply each value by a dilution factor according to Eq. (9) below where V_A, V_B, and V_C are the volumes Solutions A, B, and C, added to the cell, respectively.

$$Dilution\ \ Factor = \frac{V_A + V_B + V_C}{V_A} \tag{9}$$

Under these conditions the dilution factor is equal to $\frac{60uL + 6.68uL + 7.42uL}{60uL} = 1.235$.

11. Inspect the time trajectories of the I_{563} and I_{665} values. For PCNA loading, the appearance and increase in FRET is only confirmed by I_{563} decreasing with simultaneously increases in I_{665}. For pol δ holoenzyme formation and the initiation of DNA synthesis, a further increase in FRET is only confirmed by I_{563} decreasing further with a simultaneous and further increase in I_{665}.

Data analysis: E_{FRET} time trajectories (Fig. 7B, *Bottom*)

12. Calculate $E_{FRET,t}^{Exp}$ from the I_{563} and I_{665} values from 10.1.7. above according to Eq. (4) and plot these values as a function of time, from 0.02 to 60.03 s. The time trajectory of this E_{FRET} represents the experimental E_{FRET} trace for no interaction between Cy3-P/T DNA•RPA complexes and Cy5-PCNA. Fitting this data to a flat line yields the E_{FRET} value for the low FRET state, $\left(E_{FRET}^{\mathrm{Low}} = 0.196 \pm 2.15 \times 10^{-4}/\mathrm{s}\right.$ for Fig. 7B, *Bottom*).

13. Calculate $E_{FRET,t}^{Exp}$ from the calculated and corrected I_{563} and I_{665} values from 10.1.8. above according to Eq. (4). On the same graph from 10.1.12. above, plot these values as a function of time, from 60.03 to 410.05 s, adjusting for the dead time. E_{FRET} values observed upon the addition of Solution B to Solution A in the cell (i.e., after and including 60.03 s) are fit to Eq. (7) described above.

Summing the calculated values for $E_{\mathrm{FRET},i}$, $\mathrm{A_{inc\ 1}}$, and $\mathrm{A_{inc\ 2}}$ from the kinetic fit yields the E_{FRET} value for the high FRET state for this particular assay $\left(E_{FRET}^{High} = 0.519 \pm 0.006\right.$ for Fig. 7B, *Bottom*).

$E_{FRET,i}\left(0.197 \pm 4.33 \times 10^{-3}/\mathrm{s}\right)$ and $E_{FRET}^{Low}\left(0.196 \pm 2.15 \times 10^{-4}/\mathrm{s}\right)$ in Fig. 7B, *Bottom* are identical, again indicating that the entire E_{FRET} time trajectory observed upon the addition of Solution B to Solution A in the cell, including the dead time, can be accurately fit to a double exponential rise to determine $k_{\mathrm{obs\ inc\ 1}}$ and $k_{\mathrm{obs\ inc\ 2}}$.

14. Calculate $E_{FRET,t}^{Exp}$ from the calculated and corrected I_{563} and I_{665} values from 10.1.10. above according to Eq. (4). On the same graph from 10.1.12. above, plot these values as a function of time, from 410.05 to 760.07 s, adjusting for the dead time. E_{FRET} values observed after the addition of Solution C to the equilibrated mixture of Solutions A and B in the cell (i.e., after 410.05 s) are fit to Eq. (8) below where $E_{FRET,i}$ is the extrapolated E_{FRET} value at 410.05 s and is equal to the sum of E_{FRET}^{High} (described above) and $\mathrm{A_{inc\ 1}}\left(E_{FRET,i} = \mathrm{A_{inc\ 1}} + E_{FRET}^{High}\right)$.

$$E_{FRET,t} = E_{FRET,i} + A_{inc2}\left(1 - \mathrm{e}^{(t - 410.05s)k_{obs\ inc1}}\right) \tag{10}$$

$\mathrm{A_{inc\ 1}}$ is calculated by subtracting E_{FRET}^{High} (described above) from $E_{FRET,i}$ from the kinetic fit $\mathrm{A_{inc\ 1}} = 0.130 \pm 0.006$ for Fig. 7B, *Bottom*). Summing the calculated values for $E_{\mathrm{FRET},i}$ and $\mathrm{A_{inc\ 2}}$ from the kinetic fit yields the E_{FRET} value for the secondary high FRET state for this particular assay $\left(E_{FRET}^{High} = 0.699 \pm 4.93 \times 10^{-4}\right.$ for Fig. 7B, *Bottom*).

10.2 New approach to monitor pol δ holoenzyme formation and initiation of DNA synthesis

In the original approach described above (10.1., Fig. 7A), the initial phase of the FRET increase observed after the addition of pol δ (+dGTP) occurs within the dead time of the

assay (≤10 s) and, hence, it's observed rate constant ($k_{obs\ inc1}$) cannot be determined. The SFA-20 stopped-flow rapid kinetics accessory (Horiba) can be utilized in a new approach to selectively monitor pol δ holoenzyme formation and initiation of DNA synthesis. The new approach is detailed below and is based on 100 μL reactant volumes and a 1:1 mixing ratio (Fig. 8). The reactant volumes can be adjusted accordingly for the desired number of replicate determinations.

Experimental assay (Fig. 8)

1. Make a 100 μL solution (Solution A) containing 40 nM Cy3-P/T DNA P/T DNA, 160 nM NeutrAvidin (homotetramer), 2 mM ATP, 50 nM RPA (heterotrimer), and 40 nM RFC (heteropentamer) in 1X Mg^{2+} / Ca^{2+} Buffer (see Buffers and solutions) supplemented with 1 mM DTT and ionic strength adjusted to 200 mM by addition of appropriate volume of 500 mM KCl. Cy5-PCNA must be added last to the solution mixture to eliminate any possibility of spontaneous (i.e., non-catalyzed) loading of Cy5-PCNA onto Cy3-P/T DNA substrates. Store Solution A at room temperature, taking note of the time PCNA loading is initiated (via addition of Cy5-PCNA).
2. Make a 100 μL solution (Solution B) containing 40 nM pol δ (heterotetramer), 2 mM dGTP in 1X Mg^{2+}/Ca^{2+} Buffer (see Buffers and solutions) supplemented with 1 mM DTT and ionic strength adjusted to 200 mM by addition of appropriate volume of 500 mM KCl. Store solution B on ice.
3. Transfer Solution A to Syringe A and Solution B to Syringe B.
4. Turn on the trigger in command. After the PCNA loading reaction has been completed in Syringe B (≥5 min). Start the acquisition, recording I_{563} and I_{665}.

Data analysis

5. Plot the recorded I_{563} and I_{665} values as a function of time and inspect the time trajectories. A further increase in FRET is only confirmed by synchronized and anti-correlated changes in the time trajectories of I_{563} and I_{665} observed upon mixing of Syringe A with Syringe B. Specifically, I_{563} decreases simultaneously with increases in I_{665}.
6. Calculate $E^{Exp}_{FRET,t}$ from I_{563} and I_{665} values from 10.2.4 above according to Eq. (4) and plot these values as a function of time. Fit the $E^{Exp}_{FRET,t}$ values to Eq. (9) below.

$$E_{FRET,t} = A_{inc1}\left(1 - e^{\left(t \times k_{0bs\ inc1}\right)}\right) + A_{inc2}\left(1 - e^{\left(t \times k_{0bs\ inc2}\right)}\right) \tag{11}$$

Acknowledgments

Research summarized in the publication was supported by an award from the National Institutes of General Medical Sciences (NIGMS) of the National Institutes of Health (NIH) under award number R35 GM147238-02 (M.H.).

References

Balakrishnan L, & Bambara RA (2013). Okazaki fragment metabolism. Cold Spring Harbor Perspectives in Biology, 5(2), 185–196. 10.1101/cshperspect.a010173.

Blouin S, Craggs TD, Lafontaine DA, & Penedo JC (2009). Functional studies of DNA-protein interactions using FRET techniques. Methods in Molecular Biology, 543, 475–502. 10.1007/978-1-60327-015-1_28. [PubMed: 19378182]

Blouin S, Craggs TD, Lafontaine DA, & Penedo JC (2015). Functional studies of DNA-protein interactions using FRET techniques. Methods in Molecular Biology, 1334, 115–141. 10.1007/978-1-4939-2877-4_8. [PubMed: 26404147]

Clausen AR, Lujan SA, Burkholder AB, Orebaugh CD, Williams JS, Clausen MF, … Kunkel TA (2015). Tracking replication enzymology in vivo by genome-wide mapping of ribonucleotide incorporation. Nature Structural & Molecular Biology, 22(3), 185–191. 10.1038/nsmb.2957.

Cooper D, Uhm H, Tauzin LJ, Poddar N, & Landes CF (2013). Photobleaching lifetimes of cyanine fluorophores used for single-molecule forster resonance energy transfer in the presence of various photoprotection systems. Chembiochem: A European Journal of Chemical Biology, 14(9), 1075–1080. 10.1002/cbic.201300030. [PubMed: 23733413]

Donnianni RA, Zhou ZX, Lujan SA, Al-Zain A, Garcia V, Glancy E, … Symington LS (2019). DNA polymerase delta synthesizes both strands during breakinduced replication. Molecular Cell, 76(3), 371–381.e374. 10.1016/j.molcel.2019.07.033. [PubMed: 31495565]

Fang WH, & Modrich P (1993). Human strand-specific mismatch repair occurs by a bidirectional mechanism similar to that of the bacterial reaction. The Journal of Biological Chemistry, 268(16), 11838–11844. https://www.ncbi.nlm.nih.gov/pubmed/8505312. [PubMed: 8505312]

Fennessy RT, & Owen-Hughes T (2016). Establishment of a promoter-based chromatin architecture on recently replicated DNA can accommodate variable internucleosome spacing. Nucleic Acids Research, 44(15), 7189–7203. 10.1093/nar/gkw331. [PubMed: 27106059]

Gomes XV, Gary SL, & Burgers PM (2000). Overproduction in Escherichia coli and characterization of yeast replication factor C lacking the ligase homology domain. The Journal of Biological Chemistry, 275(19), 14541–14549. 10.1074/jbc.275.19.14541. [PubMed: 10799539]

Hedglin M, Aitha M, & Benkovic SJ (2017). Monitoring the retention of human proliferating cell nuclear antigen at primer/template junctions by proteins that bind single-stranded DNA. Biochemistry, 56(27), 3415–3421. 10.1021/acs.biochem.7b00386. [PubMed: 28590137]

Hedglin M, & Benkovic SJ (2017a). Eukaryotic translesion DNA synthesis on the leading and lagging strands: Unique detours around the same obstacle. Chemical Reviews, 117(12), 7857–7877. 10.1021/acs.chemrev.7b00046. [PubMed: 28497687]

Hedglin M, & Benkovic SJ (2017b). Replication protein A prohibits diffusion of the PCNA sliding clamp along single-stranded DNA. Biochemistry, 56(13), 1824–1835. 10.1021/acs.biochem.6b01213. [PubMed: 28177605]

Hedglin M, Kumar R, & Benkovic SJ (2013). Replication clamps and clamp loaders. Cold Spring Harbor Perspectives in Biology, 5(4), a010165–a010183. 10.1101/cshperspect.a010165. [PubMed: 23545418]

Hedglin M, Pandey B, & Benkovic SJ (2016). Stability of the human polymerase delta holoenzyme and its implications in lagging strand DNA synthesis. Proceedings of the National Academy of Sciences of the United States of America, 113(13), E1777–E1786. 10.1073/pnas.1523653113. [PubMed: 26976599]

Hedglin M, Perumal SK, Hu Z, & Benkovic S (2013). Stepwise assembly of the human replicative polymerase holoenzyme. Elife, 2, e00278. 00271–00220. 10.7554/eLife.00278.

Hoitsma NM, Norris J, Khoang TH, Kaushik V, Chadda R, Antony E, Hedglin M, & Freudenthal BD (2023). Mechanistic insight into AP-endonuclease 1 cleavage of abasic sites at stalled replication fork mimics. Nucleic Acids Research, 51(13), 6738–6753. 10.1093/nar/gkad481 [PubMed: 37264933]

Kang MS, Ryu E, Lee SW, Park J, Ha NY, Ra JS, … Myung K (2019). Regulation of PCNA cycling on replicating DNA by RFC and RFC-like complexes. Nature Communications, 10(1), 2420. 10.1038/s41467-019-10376-w.

Kemp MG, & Hu J (2017). PostExcision events in human nucleotide excision repair. Photochemistry and Photobiology, 93(1), 178–191. 10.1111/php.12641. [PubMed: 27645806]

Kim C, Paulus BF, & Wold MS (1994). Interactions of human replication protein A with oligonucleotides. Biochemistry, 33(47), 14197–14206. https://www.ncbi.nlm.nih.gov/pubmed/7947831. [PubMed: 7947831]

Kim C, Snyder RO, & Wold MS (1992). Binding properties of replication protein A from human and yeast cells. Molecular and Cellular Biology, 12(7), 3050–3059. https://www.ncbi.nlm.nih.gov/pubmed/1320195. [PubMed: 1320195]

Kim C, & Wold MS (1995). Recombinant human replication protein A binds to polynucleotides with low cooperativity. Biochemistry, 34(6), 2058–2064. https://www.ncbi.nlm.nih.gov/pubmed/7849064. [PubMed: 7849064]

Kochaniak AB, Habuchi S, Loparo JJ, Chang DJ, Cimprich KA, Walter JC, & van Oijen AM (2009). Proliferating cell nuclear antigen uses two distinct modes to move along DNA. The Journal of Biological Chemistry, 284(26), 17700–17710. 10.1074/jbc.M109.008706. [PubMed: 19411704]

Kolinjivadi AM, Sannino V, De Antoni A, Zadorozhny K, Kilkenny M, Techer H, … Costanzo V (2017). Smarcal1-mediated fork reversal triggers Mre11-dependent degradation of nascent DNA in the absence of Brca 2 and stable Rad51 nucleofilaments. Molecular Cell, 67(5), 867–881.e867. 10.1016/j.molcel.2017.07.001. [PubMed: 28757209]

Kolpashchikov DM, Khodyreva SN, Khlimankov DY, Wold MS, Favre A, & Lavrik OI (2001). Polarity of human replication protein A binding to DNA. Nucleic Acids Research, 29(2), 373–379. 10.1093/nar/29.2.373. [PubMed: 11139606]

Kolpashchikov DM, Weisshart K, Nasheuer HP, Khodyreva SN, Fanning E, Favre A, & Lavrik OI (1999). Interaction of the p70 subunit of RPA with a DNA template directs p32 to the 3′-end of nascent DNA. FEBS Letters, 450(1–2), 131–134. 10.1016/s0014-5793(99)00484-6. [PubMed: 10350071]

Lacabanne D, Wiegand T, Wili N, Kozlova MI, Cadalbert R, Klose D, … Bockmann A (2020). ATP analogues for structural investigations: Case studies of a DnaB helicase and an ABC transporter. Molecules, 25(22), 10.3390/molecules25225268.

Lancey C, Tehseen M, Raducanu VS, Rashid F, Merino N, Ragan TJ, … De Biasio A (2020). Structure of the processive human Pol delta holoenzyme. Nature Communications, 11(1), 1109. 10.1038/s41467-020-14898-6.

Li M, Sengupta B, Benkovic SJ, Lee TH, & Hedglin M (2020). PCNA mono-ubiquitination is regulated by diffusion of Rad6/Rad18 complexes along RPA filaments. Biochemistry. 10.1021/acs.biochem.0c00849.

Lujan SA, Williams JS, & Kunkel TA (2016). DNA polymerases divide the labor of genome replication. Trends in Cell Biology, 26(9), 640–654. 10.1016/j.tcb.2016.04.012. [PubMed: 27262731]

Lydeard JR, Jain S, Yamaguchi M, & Haber JE (2007). Break-induced replication and telomerase-independent telomere maintenance require Pol32. Nature, 448(7155), 820–823. 10.1038/nature06047. [PubMed: 17671506]

Maloisel L, Fabre F, & Gangloff S (2008). DNA polymerase delta is preferentially recruited during homologous recombination to promote heteroduplex DNA extension. Molecular and Cellular Biology, 28(4), 1373–1382. 10.1128/MCB.01651-07. [PubMed: 18086882]

Miyabe I, Kunkel TA, & Carr AM (2011). The major roles of DNA polymerases epsilon and delta at the eukaryotic replication fork are evolutionarily conserved. PLoS Genetics, 7(12), e1002407. 10.1371/journal.pgen.1002407. [PubMed: 22144917]

Modrich P (2016). Mechanisms in E. coli and human mismatch repair (Nobel Lecture). Angewandte Chemie (International Ed. in English), 55(30), 8490–8501. 10.1002/anie.201601412. [PubMed: 27198632]

Nguyen B, Sokoloski J, Galletto R, Elson EL, Wold MS, & Lohman TM (2014). Diffusion of human replication protein A along single-stranded DNA. Journal of Molecular Biology, 426(19), 3246–3261. 10.1016/j.jmb.2014.07.014. [PubMed: 25058683]

Nick McElhinny SA, Gordenin DA, Stith CM, Burgers PM, & Kunkel TA (2008). Division of labor at the eukaryotic replication fork. Molecular Cell, 30(2), 137–144. 10.1016/j.molcel.2008.02.022. [PubMed: 18439893]

Norris JL, Rogers LO, Pytko KG, Dannenberg RL, Perreault S, Kaushik V, … Hedglin M (2024). Replication protein A dynamically re-organizes on primer/template junctions to permit DNA polymerase delta holoenzyme assembly and initiation of DNA synthesis. Nucleic Acids Research. 10.1093/nar/gkae475.

Perumal SK, Xu X, Yan C, Ivanov I, & Benkovic SJ (2019). Recognition of a key anchor residue by a conserved hydrophobic pocket ensures subunit interface integrity in DNA clamps. Journal of Molecular Biology, 431(14), 2493–2510. 10.1016/j.jmb.2019.04.035. [PubMed: 31051173]

Pestryakov PE, Khlimankov DY, Bochkareva E, Bochkarev A, & Lavrik OI (2004). Human replication protein A (RPA) binds a primer-template junction in the absence of its major ssDNA-binding domains. Nucleic Acids Research, 32(6), 1894–1903. 10.1093/nar/gkh346. [PubMed: 15047856]

Pestryakov PE, Weisshart K, Schlott B, Khodyreva SN, Kremmer E, Grosse F, … Nasheuer HP (2003). Human replication protein A. The C-terminal RPA70 and the central RPA32 domains are involved in the interactions with the 3′-end of a primer-template DNA. The Journal of Biological Chemistry, 278(19), 17515–17524. 10.1074/jbc.M301265200. [PubMed: 12600993]

Podust VN, Tiwari N, Stephan S, & Fanning E (1998). Replication factor C disengages from proliferating cell nuclear antigen (PCNA) upon sliding clamp formation, and PCNA itself tethers DNA polymerase delta to DNA. The Journal of Biological Chemistry, 273(48), 31992–31999. 10.1074/jbc.273.48.31992. [PubMed: 9822671]

Robertson AB, Klungland A, Rognes T, & Leiros I (2009). DNA repair in mammalian cells: Base excision repair: The long and short of it. Cellular and Molecular Life Sciences: CMLS, 66(6), 981–993. 10.1007/s00018-009-8736-z. [PubMed: 19153658]

Roy R, Hohng S, & Ha T (2008). A practical guide to single-molecule FRET. Nature Methods, 5(6), 507–516. 10.1038/nmeth.1208. [PubMed: 18511918]

Schmitt MW, Matsumoto Y, & Loeb LA (2009). High fidelity and lesion bypass capability of human DNA polymerase delta. Biochimie, 91(9), 1163–1172. 10.1016/j.biochi.2009.06.007. [PubMed: 19540301]

Shibahara K, & Stillman B (1999). Replication-dependent marking of DNA by PCNA facilitates CAF-1-coupled inheritance of chromatin. Cell, 96(4), 575–585. http://www.ncbi.nlm.nih.gov/pubmed/10052459. [PubMed: 10052459]

Smith DJ, & Whitehouse I (2012). Intrinsic coupling of lagging-strand synthesis to chromatin assembly. Nature, 483(7390), 434–438. 10.1038/nature10895. [PubMed: 22419157]

Spivak G (2015). Nucleotide excision repair in humans. DNA Repair (Amsterdam), 36, 13–18. 10.1016/j.dnarep.2015.09.003.

Tims HS, & Widom J (2007). Stopped-flow fluorescence resonance energy transfer for analysis of nucleosome dynamics. Methods, 41(3), 296–303. 10.1016/j.ymeth.2007.01.001. [PubMed: 17309840]

Tsurimoto T, & Stillman B (1991). Replication factors required for SV40 DNA replication in vitro. I. DNA structure-specific recognition of a primer-template junction by eukaryotic DNA polymerases and their accessory proteins. The Journal of Biological Chemistry, 266(3), 1950–1960. http://www.ncbi.nlm.nih.gov/pubmed/1671045. [PubMed: 1671045]

Uhlmann F, Cai J, Gibbs E, O'Donnell M, & Hurwitz J (1997). Deletion analysis of the large subunit p140 in human replication factor C reveals regions required for complex formation and replication activities. The Journal of Biological Chemistry, 272(15), 10058–10064. http://www.ncbi.nlm.nih.gov/pubmed/9092549. [PubMed: 9092549]

Waga S, & Stillman B (1998). Cyclin-dependent kinase inhibitor p21 modulates the DNA primer-template recognition complex. Molecular and Cellular Biology, 18(7), 4177–4187. 10.1128/MCB.18.7.4177. [PubMed: 9632802]

Wilson MA, Kwon Y, Xu Y, Chung WH, Chi P, Niu H, … Ira G (2013). Pif1 helicase and Poldelta promote recombination-coupled DNA synthesis via bubble migration. Nature, 502(7471), 393–396. 10.1038/nature12585. [PubMed: 24025768]

Yu B, Pettitt BM, & Iwahara J (2020). Dynamics of ionic interactions at protein-nucleic acid interfaces. Accounts of Chemical Research, 53(9), 1802–1810. 10.1021/acs.accounts.0c00212. [PubMed: 32845610]

Yuzhakov A, Kelman Z, Hurwitz J, & O'Donnell M (1999). Multiple competition reactions for RPA order the assembly of the DNA polymerase delta holoenzyme. The EMBO Journal, 18(21), 6189–6199. 10.1093/emboj/18.21.6189. [PubMed: 10545128]

Zhang T, Rawal Y, Jiang H, Kwon Y, Sung P, & Greenberg RA (2023). Break-induced replication orchestrates resection-dependent template switching. Nature, 619(7968), 201–208. 10.1038/s41586-023-06177-3. [PubMed: 37316655]

Zheng X, Bi C, Li Z, Podariu M, & Hage DS (2015). Analytical methods for kinetic studies of biological interactions: A review. Journal of Pharmaceutical and Biomedical Analysis, 113, 163–180. 10.1016/j.jpba.2015.01.042. [PubMed: 25700721]

Zhou ZX, Lujan SA, Burkholder AB, Garbacz MA, & Kunkel TA (2019). Roles for DNA polymerase delta in initiating and terminating leading strand DNA replication. Nature Communications, 10(1), 3992. 10.1038/s41467-019-11995-z.

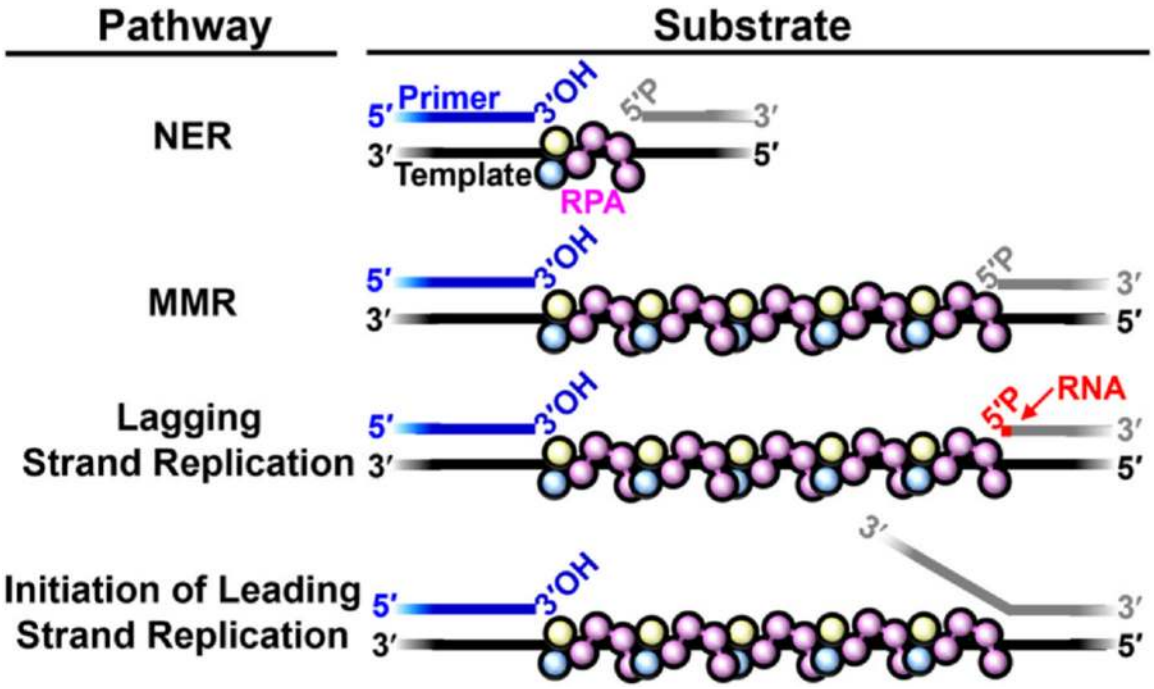

Fig. 1.

P/T DNA substrates for NER, MMR, lagging strand replication, and the initiation of leading strand replication. Each substrate contains a ssDNA ″gap″ engaged by one or more RPAs. The primer and template strands are indicated in blue and black, respectively. The complimentary DNA strands downstream of the P/T junctions, that is, non-primer strands, are shown in gray. The ″gradient″ colored portion of all DNA strands indicate continuous DNA. ″5′ P″ and 3′ OH″ indicate terminal 5′ phosphate and 3′ hydroxyl groups, respectively. RPA subunits are color-coded (RPA1 in pink, RPA2 in yellow, RPA3 in blue).

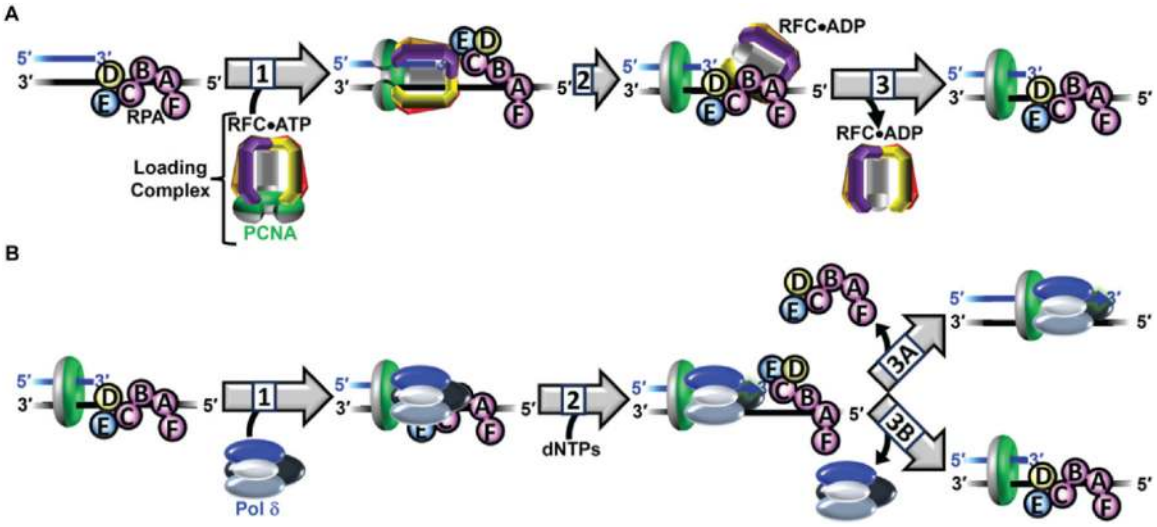

Fig. 2.

Stepwise assembly of the human pol δ holoenzyme and initiation of DNA synthesis on P/T junctions engaged by RPA. RPA subunits are color-coded (as in Fig. 1) and depicted to illustrate the oligonucleotide-bindings folds A-E. The “front” and ″back″ faces of PCNA are shown in green and gray, respectively. (A) PCNA loading. (1) Binding and activation of a loading complex at a P/T junction. (2) Hydrolysis of ATP by RFC (within activated loading complex). (3) Release of RFC•ADP into solution. (B) Initiation of DNA synthesis. (1) Formation of a pol δ holoenzyme. (2) Initiation of DNA synthesis. (3A) Processive dNTP incorporation. (3B) Dissociation of pol δ following initial dNTP incorporation. *Reprinted with permission under the terms of the Creative Commons Attribution License from Norris, J. L., Rogers, L. O., Pytko, K. G., Dannenberg, R. L., Perreault, S., Kaushik, V., … Hedglin, M. (2024). Replication protein A dynamically reorganizes on primer/template junctions to permit DNA polymerase delta holoenzyme assembly and initiation of DNA synthesis. Nucleic Acids Research, Copyright 2024 Oxford University Press*.

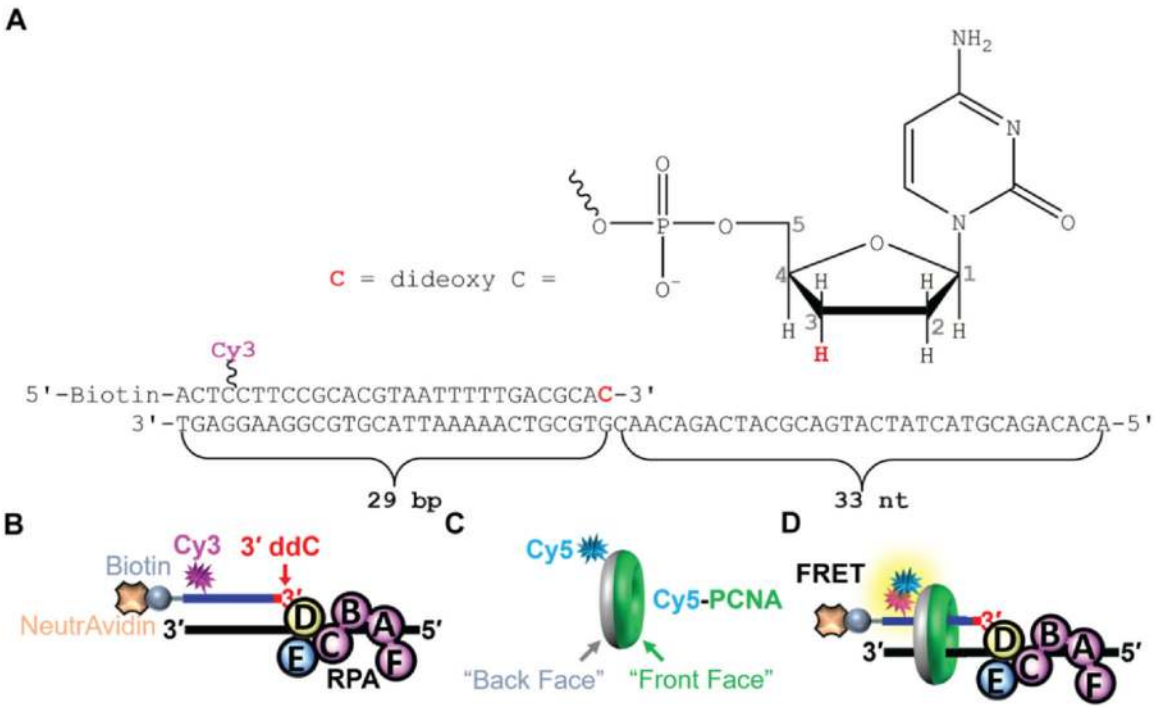

Fig. 3.

The Cy3 donor/Cy5 acceptor FRET pair. (A-B) Cy3 donor. The Cy3-labeled P/T DNA substrate (Cy3-P/T DNA) mimics a nascent P/T junction and serves as the FRET donor in the approaches described below. The structure and sequence of the Cy3-P/T DNA substrate and the structure of the 3′ terminal dideoxycytidine nucleotide of the primer strand are shown in panel (A). The Cy3-P/T DNA substrate is shown in cartoon form in panel (B), engaged by NeutrAvidin and RPA. The primer and template strands are shown in blue and black, respectively. (C) Cy5 donor. Cy5-labeled PCNA (Cy5-PCNA) serves as the FRET acceptor in the approaches described below. Cy5-PCNA is displayed in cartoon form where the ″front″ and ″back″ faces are indicated and shown in green and gray, respectively, as in Fig. 2. (D) FRET between Cy3 donor and Cy5 acceptor. When Cy5-PCNA is encircling the Cy3-P/T DNA substrate, the Cy3 donor and Cy5 acceptor are oriented towards each other, yielding FRET. Shown in cartoon form is Cy5-PCNA loaded and stabilized on the Cy3-P/T DNA substrate.

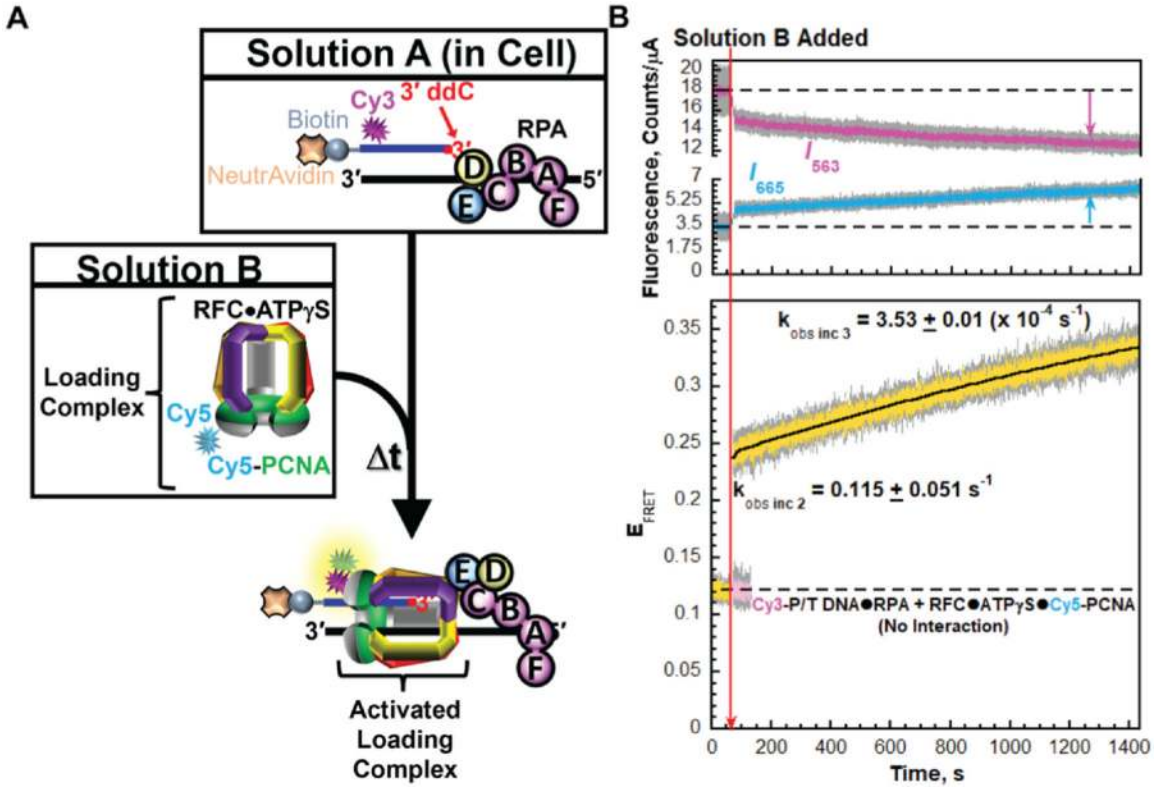

Fig. 4.

Original approach to monitor transient state kinetics of binding and activation of loading complexes via FRET. (A) Schematic representation of the experiment (B). Data. The time trajectories of I_{563} (magenta) and I_{665} (cyan) are displayed in the top panel and the corresponding E_{FRET} (mustard) is displayed in the bottom panel. The time at which Solution B is added is indicated by a red arrow. The predicted E_{FRET} trace (pink) for no interaction between Cy3-P/T DNA•RPA complexes and the Cy5-PCNA loading complexes is displayed in the bottom panel, offset to the time after the loading complexes are added. Changes in I_{563} and I_{665} are indicated in the top panel by magenta and cyan arrows, respectively. Each trace is the mean of at least three independent traces with the S.E.M. shown in gray. For observation, the I_{563} and I_{665}, and the corresponding E_{FRET} values observed prior to the addition of the loading complex are each fit to dashed flat lines that are extrapolated to the axis limits. The E_{FRET} trace observed after the addition of the loading complexes is fit to a solid double exponential rise and the observed rate constants, $k_{obs\ inc\ 2}$ and $k_{obs\ inc\ 3}$, are reported in the graph.

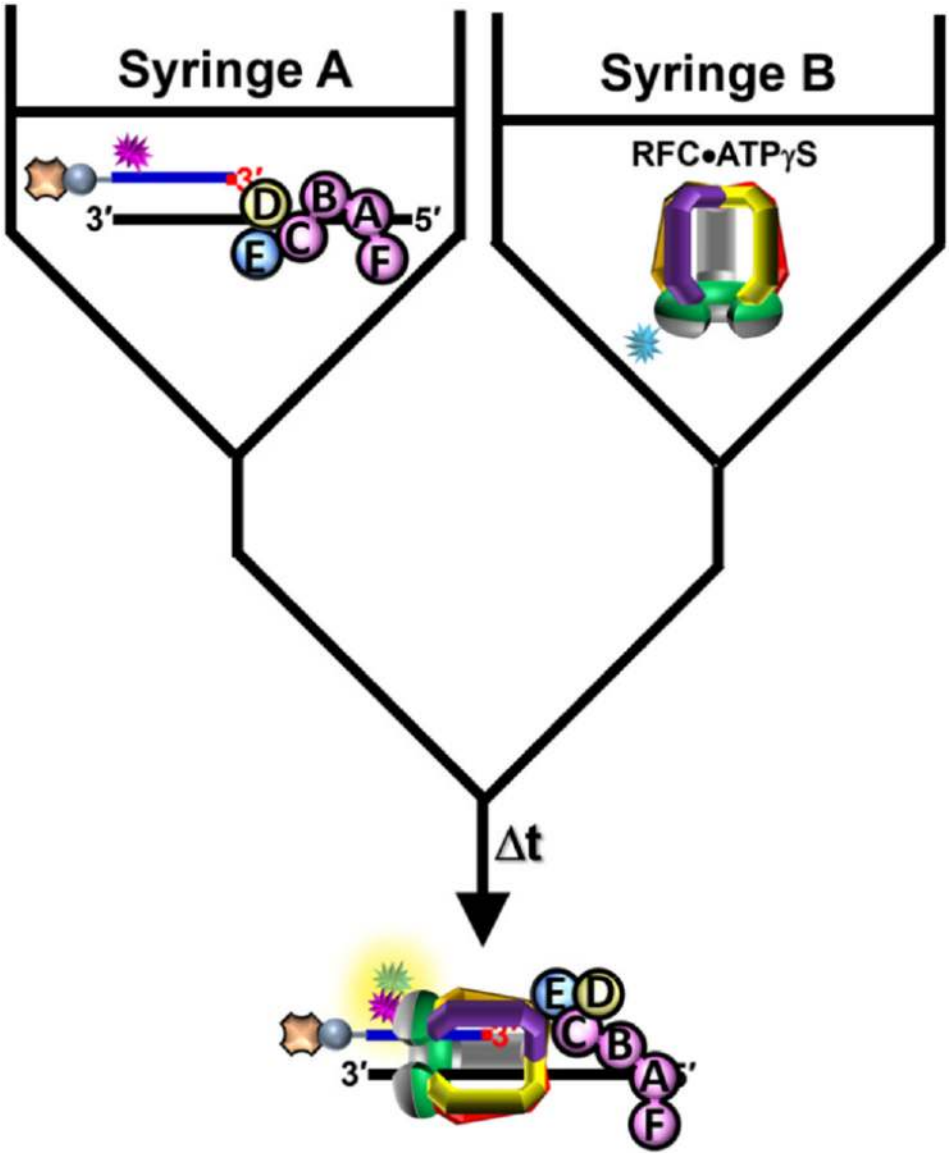

Fig. 5.

Schematic representation of new approach to monitor transient state kinetics of binding and activation of loading complexes via FRET.

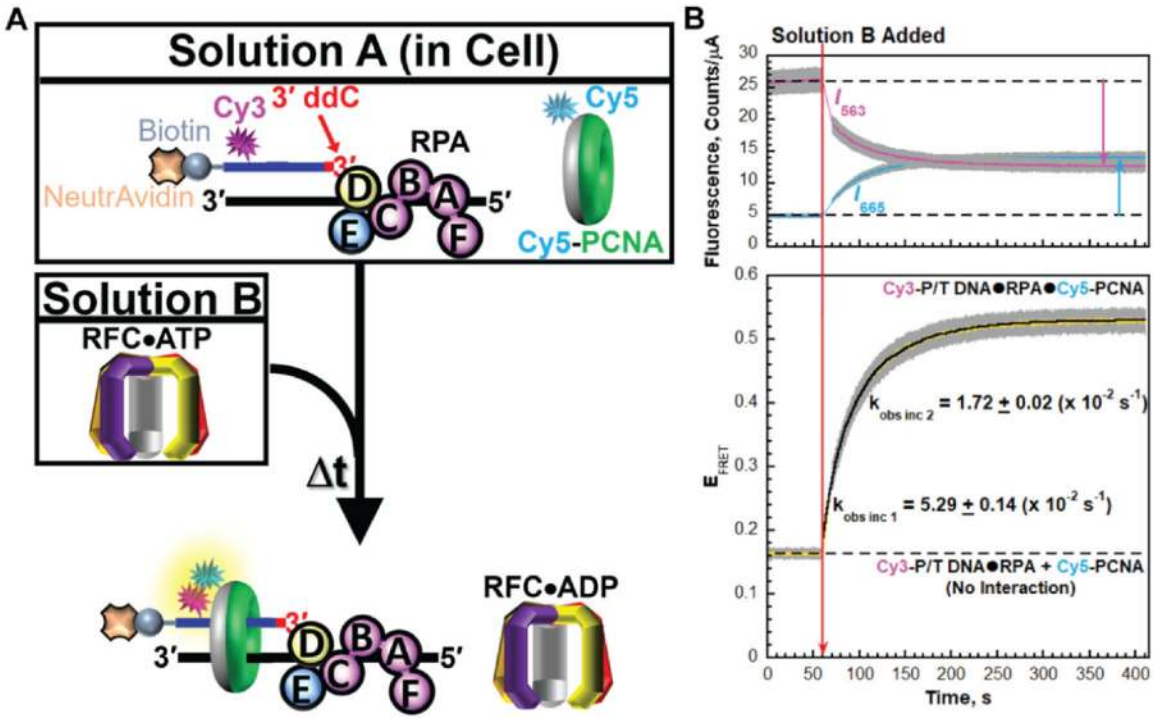

Fig. 6.

Approach to monitor transient state kinetics of PCNA loading, RFC•ADP dissociation, and repositioning of loaded PCNA via FRET. (A) Schematic representation of the experiment. (B) Data. The time trajectories of I_{563} (magenta) and I_{665} (cyan) are displayed in the top panel and the corresponding E_{FRET} (mustard) is displayed in the bottom panel. The time at which Solution B is added is indicated by a red arrow. Changes in I_{563} and I_{665} are indicated in the top panel by magenta and cyan arrows, respectively. Each trace is the mean of at least three independent traces with the S.E.M. shown in gray. For observation, the I_{563} and I_{665}, and the corresponding E_{FRET} values observed prior to the addition of the RFC•ATP complexes are each fit to dashed flat lines that are extrapolated to the axis limits. The E_{FRET} trace observed prior to the addition of RFC•ATP complexes (in the bottom panel) represents the complete absence of interactions between the Cy3-P/T DNA•RPA complexes and Cy5-PCNA. The E_{FRET} trace observed upon the addition of the RFC•ATP complexes (in the bottom panel) is fit to a solid double exponential rise and the observed rate constants, $k_{obs\ inc\ 1}$ and $k_{obs\ inc\ 2}$, are reported in the graph.

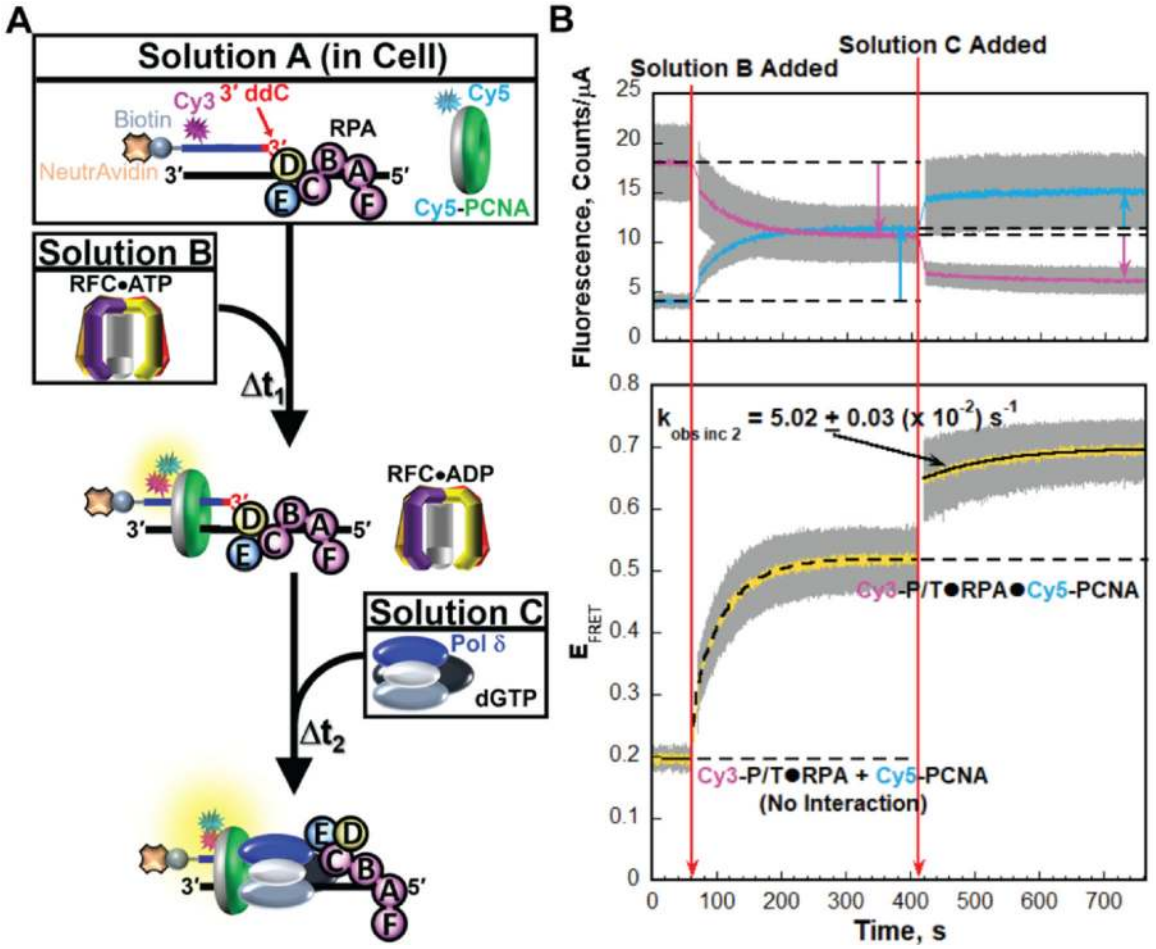

Fig. 7.

Monitoring transient state kinetics of pol *δ* holoenzyme formation and initiation of DNA synthesis via FRET. (A) Schematic representation of the experiment. (B) Data. The time trajectories of I_{563} (magenta) and I_{665} (cyan) are displayed in the top panel and the corresponding E_{FRET} (mustard) is displayed in the bottom panel. The times at Solutions B and C are added are indicated by red arrows. Changes in I_{563} and I_{665} are indicated in the top panel by magenta and cyan arrows, respectively. Each trace is the mean of at least three independent traces with the S.E.M. shown in gray. For observation, the I_{563} and I_{665}, and E_{FRET} values observed prior to the addition of the RFC•ATP complexes are fit to dashed flat lines that are extrapolated to the time at which pol *δ* (+ dGTP) is added. The E_{FRET} trace observed prior to the addition of RFC•ATP complexes (in the bottom panel) represents the complete absence of interactions between the Cy3-P/T DNA•RPA complexes and Cy5-PCNA. For observation, dashed flat lines are drawn to highlight the plateau / values observed after the addition of RFC•ATP complexes (in the top panel).The E_{FRET} trace observed upon the addition of the RFC•ATP complexes (in the bottom panel) is fit to a dashed double exponential rise that is extrapolated to the axis limits. The plateau E_{FRET} values observed after the addition of RFC•ATP complexes (in the bottom panel) represents loading and stabilization of Cy5-PCNA on all Cy3-P/T DNA substrates. The E_{FRET} traces observed after

the addition of pol δ (+dGTP) (in the bottom panel) is fit to a solid single exponential rise and the observed rate constant, $k_{\text{obs inc 2}}$, is reported in the graph.

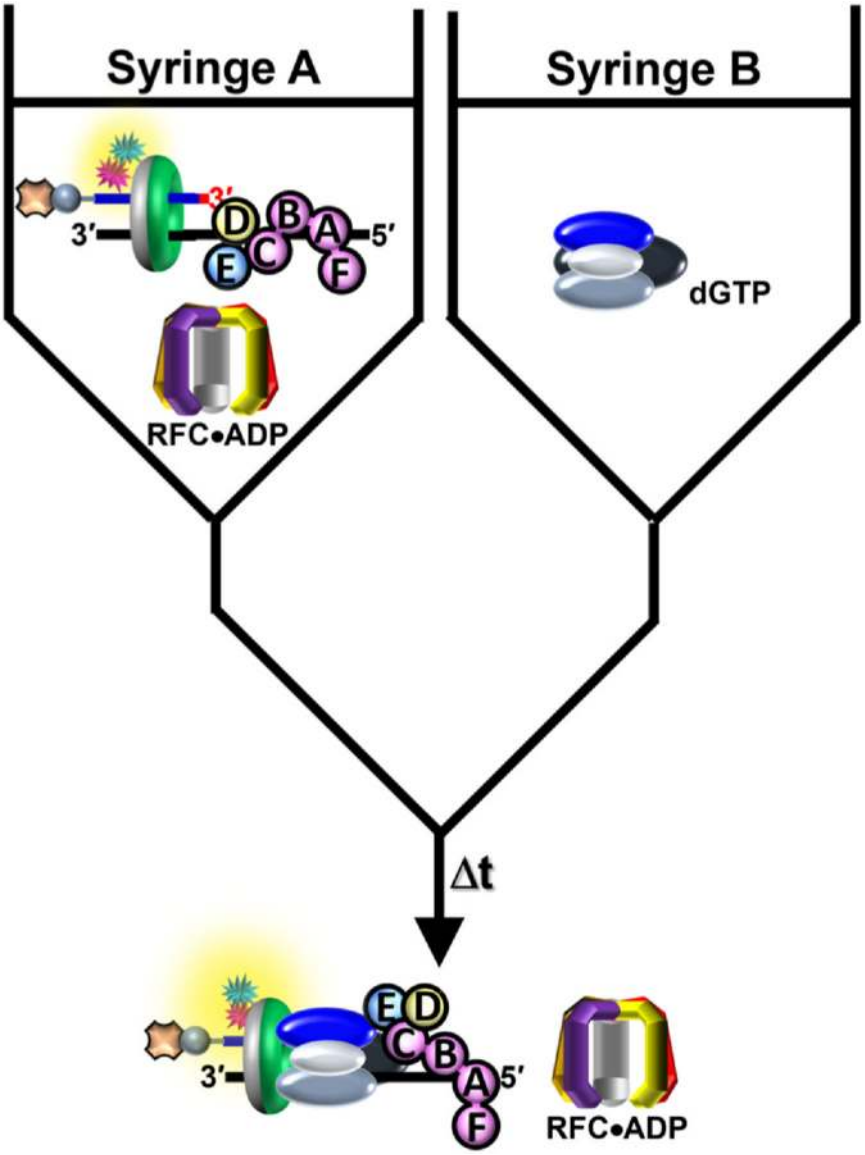

Fig. 8.

Schematic representation of new approach to monitor pol *δ* holoenzyme formation and initiation of DNA synthesis via FRET.